HAL open science

Assessment of six soil ecosystem services by coupling simulation modelling and field measurement of soil properties

Yosra Ellili-Bargaoui, Christian Walter, Blandine Lemercier, Didier Michot

To cite this version:

Yosra Ellili-Bargaoui, Christian Walter, Blandine Lemercier, Didier Michot. Assessment of six soil ecosystem services by coupling simulation modelling and field measurement of soil properties. Ecological Indicators, 2021, 121, pp.107211. 10.1016/j.ecolind.2020.107211 . hal-03160523

HAL Id: hal-03160523

https://hal.science/hal-03160523v1

Submitted on 28 May 2021

HAL is a multi-disciplinary open access archive for the deposit and dissemination of scientific research documents, whether they are published or not. The documents may come from teaching and research institutions in France or abroad, or from public or private research centers.

L'archive ouverte pluridisciplinaire **HAL**, est destinée au dépôt et à la diffusion de documents scientifiques de niveau recherche, publiés ou non, émanant des établissements d'enseignement et de recherche français ou étrangers, des laboratoires publics ou privés.

Ecological Indicators 121 (2021) 107211

Contents lists available at ScienceDirect

Ecological Indicators

journal homepage: www.elsevier.com/locate/ecolind

Assessment of six soil ecosystem services by coupling simulation modelling and field measurement of soil properties

Yosra Ellili-Bargaoui [a,b,*], Christian Walter [a], Blandine Lemercier [a], Didier Michot [a]

[a] UMR SAS, Institut Agro, INRAE, 35000 Rennes, France
[b] Interact, UniLaSalle, 60000 Beauvais, France

ARTICLE INFO

Keywords:
Soil ecosystem services
STICS
Biophysical indicators
Provisioning ecosystem services
Regulating ecosystem services

ABSTRACT

Soil is a reservoir of natural capital that provides several ecosystem services, ensuring human well-being and sustainable socioeconomic development. Many researchers nevertheless argue that there is no consensus on practical indicators to assess soil ecosystem services (SES). As many policy decisions rely on metrics and indicators to communicate concise and relevant information, an assessment of ecosystem service indicators can help identifying gaps hindering policymakers from more fully adopting ecosystem service approaches. The aim of this study was to develop a method to quantitatively evaluate six SES using a set of indicators derived from dynamic soil and crop modelling using the STICS model developed by INRA. In a 6 775 km^2 study area in north-western France (Brittany), 64 soil sampling points, located in agricultural areas, were selected following a stratified random sampling design based on soil parent material stratification. STICS inputs required climate data, soil property data and soil and landscape management practices. Over a baseline period from 1988 to 2018, similar crop management practices were simulated that reflected the dominant one performed by conventional farmers across the study site: applying organic and mineral fertilizers to a maize-wheat-catch crop rotation. Also, STICS outputs were used to derive six biophysical indicators characterizing six SES. Both mean and annual SES indicators were calculated and analyzed. Interrelations among SES indicators and soil properties were investigated using a Pearson correlation matrix, multivariate variance analysis and regression-based methods. The main results revealed that pedological and inter-annual variability were the main drivers of SES provision, particularly for ground water recharge, plant biomass provision, plant water provision and carbon sequestration. All SES were strongly correlated, except carbon sequestration and plant nitrogen provision, which showed weak correlations with the rest of SES. Moreover, analyzing interrelations between SES indicators and soil properties such as soil depth, soil texture and its related variables such as available water capacity played a predominant role in ensuring high levels of water-related SES indicators. Meanwhile, physicochemical soil properties were strongly correlated with carbon sequestration but less so with plant nitrogen provision. Overall, these findings characterize the effect of soil variability on SES provision using modelling and field measures of several soil properties, which can be useful for policy makers.

1. Introduction

Soils provide a wide range of goods and services important for human well-being and sustainable socio-economic development, collectively called "ecosystem services" (Costanza et al., 1997). The ecosystem services concept emerged in economics in 1970 (Cardona, 2012) and was considered the central pillar of the Millennium Ecosystem Assessment (MEA) in 2005 (Millennium Ecosystem Assessment, 2005).

The conceptual framework for classifying, quantifying and modelling ecosystem services is often context-specific. In the literature, three main international classifications are widely used: the MEA (2005), The Economics of Ecosystems and Biodiversity (TEEB, 2010) and the Common International Classification of Ecosystem Services (CICES, 2013). For the first two frameworks, four primary categories of services are distinguished: provisioning (e.g. fresh water, wood, food, and fibre), regulating (e.g. climate, erosion, and floods), cultural (e.g. aesthetic or spiritual values) and supporting (e.g. physical support to plants, animals and human infrastructure). However, the CICES framework distinguishes only provisioning, regulating and cultural categories

* Corresponding author at: Interact, UniLaSalle, 60000 Beauvais, France.
E-mail address: Yosra.ellili@unilasalle.fr (Y. Ellili-Bargaoui).

https://doi.org/10.1016/j.ecolind.2020.107211
Received 12 June 2020; Received in revised form 16 November 2020; Accepted 22 November 2020
Available online 8 December 2020
1470-160X/© 2020 The Author(s). Published by Elsevier Ltd. This is an open access article under the CC BY-NC-ND license (http://creativecommons.org/licenses/by-nc-nd/4.0/).

and considers therefore that cultural services are included in the regulation category.

Soil is defined as the central interface between the lithosphere, biosphere, hydrosphere and atmosphere (Dominati et al., 2014; Greiner et al., 2017; Szabolcs, 1994). Understanding the multifunctional role of soil in ecosystem functioning is crucial (Bouma, 2010, 2014; Dominati et al., 2014), and more importance was recently accorded in soil science research to quantifying soil's contribution to human welfare. Due to its inherent and manageable properties and processes, soil ensures specific functions that set a biological balance among ecosystem components. The conceptual framework of Dominati et al. (2010) considers the soil as natural capital with stocks of matter and biodiversity, but also with generated flows, allowing the provision of several services fulfilling human needs. Robinson et al. (2012), Egoh et al., 2008, and McBratney et al. (2014) emphasized the need to assess soil ecosystem services (SES) and promote soil-ecosystem connections when developing land-resource policy and management. In the scientific literature, however, assessment of SES, based on fundamental soil features, is rarely investigated or defined (Adhikari and Hartemink, 2016).

Currently, one of the greatest challenges is how to quantify SES (Adhikari and Hartemink, 2016; Baveye et al., 2016; Costanza et al., 1997; de Groot et al., 2010; Hauck et al., 2016). In general, biophysical assessment is performed using indicators (also called "metrics") (Hauck et al., 2016). Direct measurement of SES consists of measuring soil properties and processes involved in each SES. For instance, the soil's contribution to climate regulation is assessed mainly by its ability to sequester organic carbon in topsoil horizons (Baveye et al., 2016; Ellili et al., 2019); even if some studies suggest that deeper soil horizons can also contribute significantly to carbon sequestration (Calzolari et al., 2016). To characterise dynamics of soil organic carbon (SOC) over time, resampling soils and correctly interpreting observed changes in SOC are mandatory. Monitoring these changes is hampered, however, by several sources of uncertainty, which are related mainly to land-use change and agricultural practices that greatly influence soil bulk density and SOC content.

In contrast, modelling consists of mathematically describing soil processes that underlie the provision of SES (Nelson et al., 2009). Soil properties that are key to providing a particular SES are identified and related to context-specific environmental variables. Thus, SES assessment can benefit from soil research into dynamic spatio-temporal modelling of soil properties and processes that can support provision of SES (Adhikari and Hartemink, 2016; Calzolari et al., 2016). For instance, several studies have quantified water-quality regulation service by modelling water percolation and the associated filtration of pollutants (Baveye et al., 2016). Other researchers have estimated soil erosion regulation by combining the Universal Soil Loss Equation (USLE) and the Soil and Water Assessment Tool (SWAT) (Francesconi et al., 2016). Moreover, at the French national scale, the EFESE-EA "Evaluation Française des Ecosystèmes et des Services Ecosystémiques-Ecosystémes Agricoles" collective expertise has attempted to assess several SES using the STICS ("Simulateur mulTIdisciplinaire pour les Cultures Standard") dynamic model developed by INRA (Brisson et al., 2003). Essentially, a wide range of provisioning, regulation and cultural SES were assessed over a wide range of pedoclimatic variability and under different management scenarios. Their results pointed out that the high pedological variability, occurring at the national scale, generated a high variability in SES supply. Obtained results were closely linked to the crops spatial distribution as well as their temporal distribution over crop rotations (EFESE-EA, 2017). The collective expertise also identified the major trends between SES and their potential drivers e.g. N and water, fertilization and irrigation practices and agricultural production levels.

As modelling ecosystem services requires many input variables, direct measurements are recommended (Baveye et al., 2016); however, they are rarely used in the literature because of a lack of soil data (Adhikari and Hartemink, 2016). To compensate for the lack of soil data, several studies have used proxies, which play an important role in spatial planning of SES. The proxy approach consists of using certain environmental variables and soil properties to quantify SES indirectly. The most commonly used proxies are land-use and land-cover data (Adhikari and Hartemink, 2016), which have been useful in regions where soil data are scarce (Vrebos et al., 2015). These data are used as indicators of ecosystem services and properties, and to estimate the spatial provision of ecosystem services. In several landscapes from Colombia and Brazil, Grimaldi et al. (2014) quantified water cycle and soil erosion regulation services using the rate of water infiltration into the soil. Similarly, Calzolari et al. (2016) assessed eight ecosystem services at the regional scale in Italy by creating multiple indices based on both manageable and inherent soil properties, which are available from legacy soil data. Furthermore, the benefits-transfer approach, based on the spatial distribution of proxies, is widely used to generate maps of ecosystem services (Nelson et al., 2009). This method uses "broad-scale assessments" (Nelson et al., 2009) to extrapolate from point estimates of multiple services to the entire biosphere (Costanza et al., 1997; Nelson et al., 2009). This approach dismisses the spatial heterogeneity of ecosystem services that depend on agricultural practices and local environmental context (Costanza et al., 1997; Nelson et al., 2009).

Despite the large number of studies on biophysical assessment of SES, there is currently no standard or widely recognised method that correctly defines and quantifies each service (Adhikari and Hartemink, 2016; Drobnik et al., 2018; Greiner et al., 2017; Maes et al., 2012). Researchers continue to develop indicator frameworks, which remain a great challenge because of the lack of normative guidelines for selecting ecosystem service indicators (Hauck et al., 2016). For instance, to represent the climate regulation ecosystem service, Grimaldi et al. (2014) used the SOC stock of the 0–30 cm layer on a given date as an indicator while, for the same purpose, Nelson et al. (2009) selected the change in SOC stock over time.

Several studies have attempted to describe relationships among ecosystem services because identifying and understanding the former are crucial for decision makers and stakeholders (Hauck et al., 2016; Nelson et al., 2009; Wu et al., 2013). Understanding SES interrelations offers a relevant support for landscape managers to guide their choices when knowledge about landscape functions is lacking (Fossey et al., 2020). Moreover, knowledge about SES interactions contribute to defining and evaluating policies. For instance, it may help to identify awareness about environmental issues and foster dialogue among stakeholders. According to Bennett et al. (2009), interactions among ecosystem services reveals two types of interactions: synergy and trade-off. Synergy involves mutual improvement of ecosystem services. Thus, benefits of one ecosystem service directly increase those of another service. In contrast, trade-off refers to decreasing one ecosystem service while increasing another. Following a general use, we distinguished three possible interactions: trade-off, synergy and no effect (Bennett et al., 2009; Jopke et al., 2015; Lee and Lautenbach, 2016).

In the literature, various methods exist to quantify these interactions using empirical methods, econometric tools, scenario simulations and participatory methods (Deng et al., 2016; Díaz et al., 2018; Lee and Lautenbach, 2016; Nelson et al., 2009). In 2014, Mouchet et al. explicitly identified a set of quantitative methods to assess interrelations among ecosystem services, describing most methods with their potential framework application. Of these methods, pairwise correlation coefficients are the most popular quantitative method to assess interactions among ecosystem services. Regression-based methods address more mechanistic relationships among SES. Other multivariate analyses were identified as being more flexible, regardless the nature of the ecosystem service indicator, such Principal Component Analysis (PCA), Factorial Analysis for Mixed Data and Redundancy Analysis. Another promising tool, Structural Equation Modelling (Grace, 2006), was also identified as a relevant way to investigate causal relationships among ecosystem services, ecosystem properties and a set of explanatory variables. Ecosystem service interactions can be also visualised using radial

diagrams (Egoh et al., 2008; Calzolari et al., 2016), and bagplots were used (Jopke et al., 2015) to map SES interactions at the European scale.

The purpose of this study was to assess SES and interrelations in the dominant agricultural system of western France using the STICS model over a period of 30 years. Six SES were selected: two regulating SES (climate regulation (CS) via soil carbon sequestration and water quality regulation (WQ)), and four provision SES: groundwater recharge (GW), water to plant provision (WP), nitrogen (N) to plant provision (NP) and plant biomass provision (YE). These six SES were assessed at 64 observation sites covering the primary soil variability observed in Brittany (France). We explored the influence of inter-annual climatic variability and pedological variability on SES, as well as interrelations between SES to highlight synergy and trade-off situations. Furthermore, interrelations between SES and some soil properties were also investigated to determine the soil properties that most influence the provision of each SES.

2. Materials and methods

2.1. The study area

The study area is the Ille-et-Vilaine department, in eastern Brittany (NW France, 47° 40′ to 48° 40′ N, 1° to 2° 20′ W). It covers an area of 6 775 km2 with gentle topographic features, except in the western zone, where the elevation peaks at 256 m. The study area is part of the Armorican Massif (BRGM, 2009), whose geology is complex: intrusive rocks (granite, gneiss and micaschist) in northern and north-western zones, sedimentary rocks (sandstone, Brioverian schist) in central and southern zones, and superficial deposits (loess, alluvial and colluvium deposits) overlaying bedrock formations with decreasing thickness from north to south (INRA Infosol, 2014). This high geological heterogeneity generates high soil variability over short distances. Most soils in the study area are Leptosols, Cambisols, Luvisols and Stagnic Fluvisols according to the World Reference Base of Soil Resources (IUSS Working Group WRB, 2014). In specific locations, Podzols, Histosols and Tidalic Fluvisols are observed. Agriculture in the study area is devoted mainly to milk and animal production, and the major crops (wheat, maize and barley) are used for animal feed.

2.2. The STICS soil-crop model

In this study, we used the STICS crop model (Brisson et al., 2003), which was designed to simulate simultaneously crop growth and several soil processes connecting water, N and carbon dynamics in the soil-crop-atmosphere continuum. STICS is one-dimensional model with a daily time step for multi-year simulations. It distinguishes multiple compartments of the crop canopy and defines a soil profile with at most five layers. STICS has been calibrated for several crops such as maize and wheat (Brisson et al., 2003) and soybean (Marraccini et al., 2020). It has been used in several countries, such as Portugal (Fraga et al., 2018) and Brazil (Silva et al., 2019). The French collective expertise EFESE-EA selected STICS to assess several SES at the French national scale under different management scenarios, soil water conditions and irrigation regimes (EFESE-EA, 2017).

More precisely, STICS simulates the effect of water and nitrogen stress on leaf area index (LAI), carbon assimilation, aerial biomass, root development and harvest index. Evapotranspiration and N uptake are assessed based on the concept of limiting factor between soil supply and plant demand.

In STICS model, water storage capacity considers porosity of fine soil and stony materials. STICS model is a capacitative type model which based on the water storage capacity (i.e. the difference between the water contents at field capacity and at wilting point). Water percolation occurs when water content exceeds field capacity. N leaching down a soil profile is simulated using the 'mixing cells' concept which accounts for convection and dispersion.

N dynamics are simulated by distinguishing three compartments of soil organic matter: the fresh organic matter (FOM) including crop residues and organic amendments, the microbial biomass, and the humified organic matter (SOM) which is devised into a stable and an active compartment. The C/N ratio characterizes FOM, which is derived from the scientific literature and long-term monitoring networks. The N mineralization from SOM depends on water content and soil temperature and soil potential mineralization rate. This latter variable depends on organic N content, soil bulk density, clay content, CaCO3 content, and thickness of the biologically active layer for mineralization (profhum).

The STICS model also considers agricultural practices like soil tillage, organic and mineral fertilization schedules and irrigation conditions. By carrying out successive simulations, the decomposition of added organic residues is simulated over the study period. A detailed description about the STICS model can be found in Beaudoin et al. (2008).

As regard STICS input data, the model requires several parameters, which remain constant throughout each simulation (like textural variables and soil depth) and a set of variables which change over time (like soil moisture and groundwater level). For soil variables, STICS requires the C/N ratio, the clay content and the pH of the top soil layer. For each soil horizon, the bulk density of fine soil, the water contents respectively at permanent wilting point and field capacity as well as their thickness must be provided. Other variables including the profhum, maximum rooting depth (obstarac) should also be defined accurately given to characterize the overall soil profile behavior.

2.3. Datasets

2.3.1. Climate dataset

Climatic conditions were assumed to be spatially uniform over the study area, and the daily input data required for the model were obtained from the meteorological station of Saint-Jacques-de-la-Lande, near Rennes, located 100 m above sea level. Daily weather variables were retrieved for the baseline period 1988–2018 from the INRA CLIMATIK weather database (INRA, 2019). Data included daily precipitation (mm), solar radiation (MJ m^{-2}), mean daily wind speed (m s^{-1}), maximum and minimum air temperature (°C) and relative air humidity (%). Potential evapotranspiration (mm day^{-1}) was estimated by the Penman-Monteith method. Fig. 1 shows the mean annual rainfall, global solar radiation and the mean annual temperature over the baseline period.

2.3.2. Soil dataset

In a previous study (Ellili Bargaoui et al., 2019), 135 soil profiles were sampled over the 6 775 km^2 study area following a stratified random sampling design based on an existing 1:250,000 soil parent material map (Fig. 2). The soils were augered down to 2 m or to paralithic contact, and their morphology was described in detail to relate the soil type to the French Référentiel Pédologique (Baize and Girard, 2008) and to the WRB international classification (IUSS, 2014). The profiles were then sampled at six regular depths according to *GlobalSoilMap* specifications (0–5, 5–15, 15–30, 30–60, 60–100, and 100–200 cm) (Ellili-Bargaoui et al., 2020; Arrouays et al., 2014). Of the 135 soil profiles, data of 64 sites located on agricultural land were used for this study. To decrease costs, only three soil layers (5–15, 30–60 and 100–200 cm) were analysed. All soil samples were analysed according to standard methods to determine their SOC content by dry combustion (Thermoscientific Finnigan EA 1112 Flash elemental analyser) (NF ISO 10694), soil mineral N content, cation exchange capacity (CEC) (NFX 31–130), pH 1:5 H_2O (soil pH in water with 1:5 soil-to-water ratio, NF ISO 10390) and their particle size distribution in three classes (clay, silt, and sand, NF X 31–107). The volumetric stony material percentage was also determined after soil samples were air-dried and sieved to 2 mm. Table 1 describes the input soil STICS variables for six soil profiles reflecting the pedological diversity occurring over the study area. The

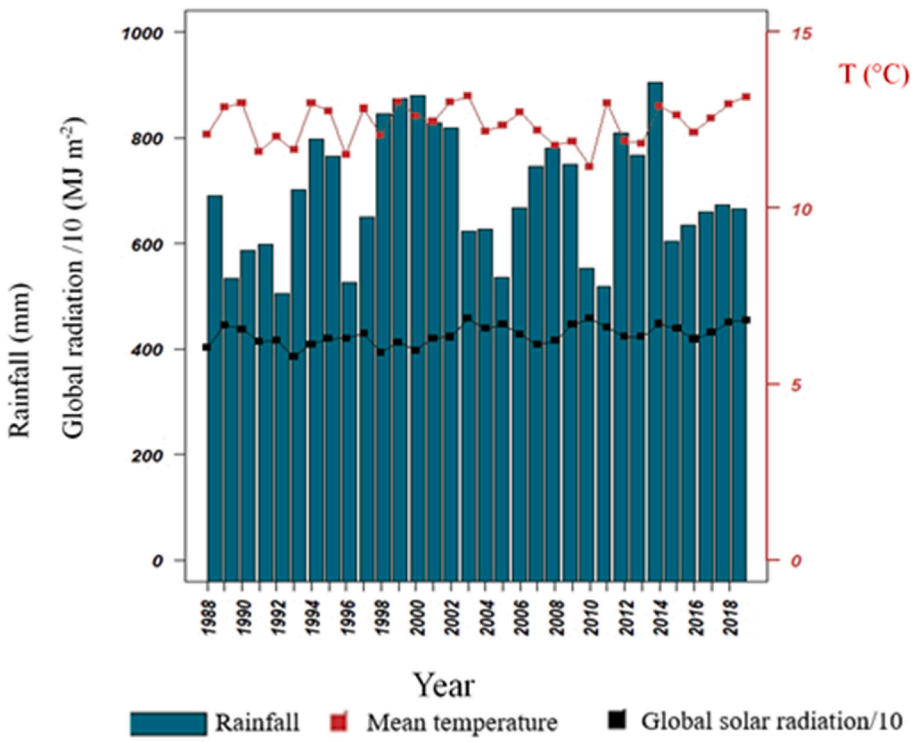

Fig. 1. Mean annual rainfall (mm), global solar radiation (MJ m-2) and mean annual temperature (°C) of the study area.

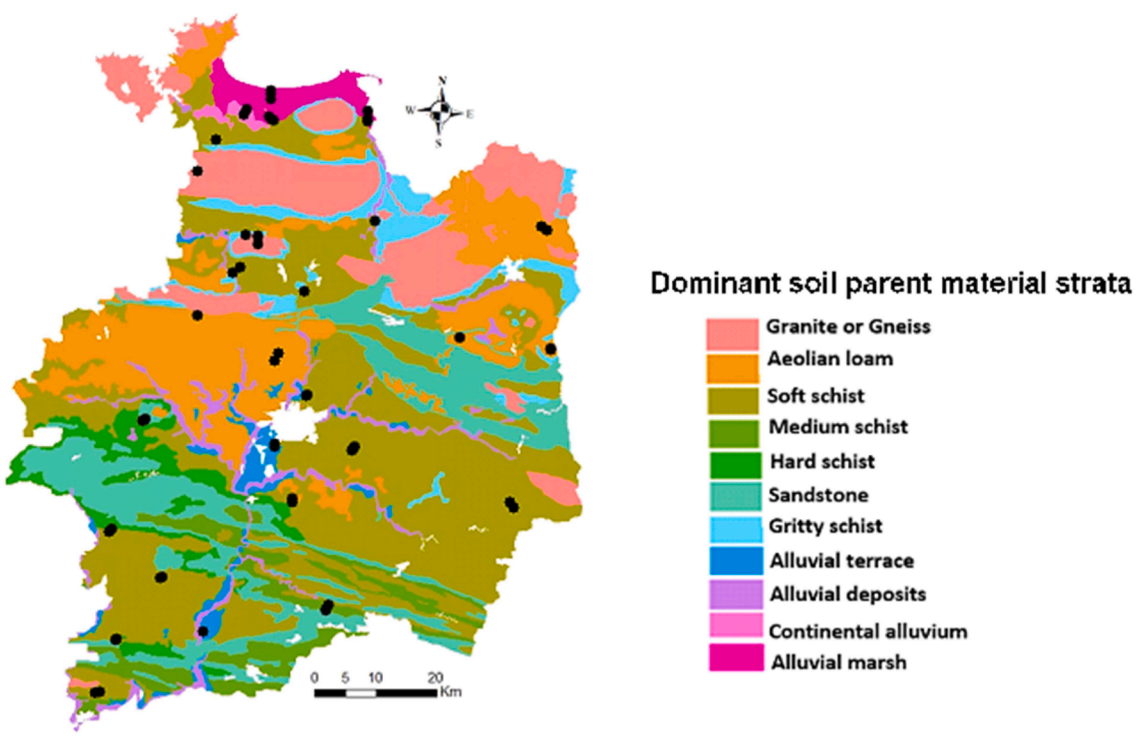

Fig. 2. Location of the 64 soil sites selected by stratified simple random sampling based on dominant soil parent strata (Ellili Bargaoui et al., 2019).

six sites were selected by ranking the 64 sites by increasing soil depth then retaining every ten sites.

Additional soil characteristics required to parameterise STICS were derived either from tables in the STICS manual (Baumont et al., 2010) or measurements performed in the study area. Soil physical characteristics, such as water content at field capacity, permanent wilting point and bulk density of fine earth, were estimated using local pedotransfer functions based on soil property analyses of >500 representative soil samples (Remy et al., 2015) (Table 1).

The thickness of the biologically active layer for mineralization and carbon dynamics was set to 30 cm. The maximum rooting depth, which depends strongly on soil type, was set to the depth of the top of the C

Table 1
Characteristics of six representative soil profiles in the dataset of 64 sampling points based on soil analyses and estimates used as input parameters for the STICS model.

[a]Soil type		G30a		L61a		N86b	O22a		T121b		Vcm2c	
Depth		0–30	30–40	0.30	90–100	0–30	0–25	40–48	0–30	50–70	0–32	75–100
[b]*Soil*												
Clay	%	16.50		13.4		23.4	21.3		13.60		37.4	
Organic C	%	0.15		0.19		0.26	0.21		0.11		0.11	
Organic N	%	11.03		10.10		9.84	10.7		10.78		11.02	
pH (water)		6.04		6.51		5.72	6.34		5.55		7.36	
W_{FC}	%	23.42	17.2	29.15	22.87	29.91	29.83	25.13	22.66	20.09	45.45	44.31
W_{Wp}	%	12.05	8.1	12.3	10.57	16.54	15.48	13.64	10.26	10.00	28.74	27.20
Bulk density	g cm^{-3}	1.27	1.43	1.24	1.49	1.24	1.24	1.34	1.33	1.46	1.24	1.24
Stones	%vol	21.46	37	2.16	5.11	36.34	18.3	37.22	3.06	15.01	0.00	1.14
[c]*STICS parameters*												
Profhum	cm	30		30		30	30		30		30	
Obstarac	cm	40		100		30	48		70		100	

[a] Soil types: G30a = Dystric Cambisol developed from granite with a depth of 30 cm; L61a = Endostagnic Cambisol on deep loam with a depth of 150 cm; N86b = Leptosol developed from soft schist with a depth of 30 cm; O22a = Cambisol developed from medium schist with a depth of 48 cm; T121b = Cambisol on an alluvial terrace with a depth of 70 cm; and Vcm2c = Histosol developed on marsh with a depth of 220 cm
[b] Soil analyses: WFC = water content at field capacity, WWP = water content at permanent wilting point.
[c] STICS parameters: profhum = biologically active soil depth for mineralisation; obstarac = maximum rooting depth.

horizon for shallow soils and 100 cm for soils deeper than 100 cm (Table 1). For each soil layer, water infiltration rate was set to a default value of 50 mm per day.

2.3.3. Crop management

Crop management was simulated based on the dominant practices performed by conventional farmers in the Ille-et-Vilaine department. Requirements of the European Union Nitrates Directive, revised in 2014 (EC, 2013), were considered to define the amounts of organic and mineral N inputs. Over the baseline period, the same maize-wheat-catch crop rotation was simulated with fixed annual sowing and soil-tillage dates and organic and mineral fertilization schedule. The crop rotation simulated lasts two years and has three successive crops (Fig. 3):

- The grain maize crop was grown from 10 April to 30 October (harvest) in the first year of each rotation. Before sowing maize, soils were ploughed to ca. 25 cm and 35 t ha^{-1} of pig slurry was applied. A semi-early maize variety (DK 250) was sown on 15 April with a planting density of 10 plants m^{-2}. To avoid delayed germination due to potential drought conditions in the topsoil, 15 mm of water was provided by irrigation at sowing. Maize was fertilised with 100 kg ha^{-1} of ammonium nitrate 30 days after planting. After harvest, stubble and roots were left on the field as crop residues, and the aboveground biomass was exported.
- The winter wheat crop was grown after the maize crop, from 1 November of the first year of the rotation to 31 July (harvest) of the second year. As simulations were run sequentially over the baseline period, the final crop residues and the soil water content of the maize crop simulation were used to initialize the carbon, N and water balances of the wheat crop simulation. Before sowing wheat, soils were ploughed to a depth of 25 cm then sown at a density of 311 plants m^{-2}. The crop was fertilized with 40 t ha^{-1} of pig slurry on 15 March, followed 70 kg ha^{-1} of ammonium of nitrate on 15 May. After harvest, aboveground biomass as well as crop residues were exported.
- The catch crop (white mustard) was grown between the winter and spring crops, as required by regulations. The cover crop was sown on 5 September and ploughed into the soil on 3 March as crop residues, one month before sowing the following maize crop.

2.4. Simulation procedure

The crop rotation was simulated with the latest version of STICS (v9.0) and its parameter sets. Over the study period (1988–2018), soil parameters remained static except for carbon, N and water in soil layers, under the influence of dynamic climatic conditions and crop growth. To initialize the STICS model, we carried out several simulations over three extra years 1985, 1986, 1987. Because the three cropping periods of the rotation were run sequentially, simulation *n* was initialised with results of simulation *n-1*. By combining soil characteristics of the 64 sites sampled, and crop rotations identified over the 30 year-period, 3565 STICS simulations were performed by using a Java package developed in this study to automate simulations. STICS provides >200 outputs, some of which describe daily values of soil properties, such as the water

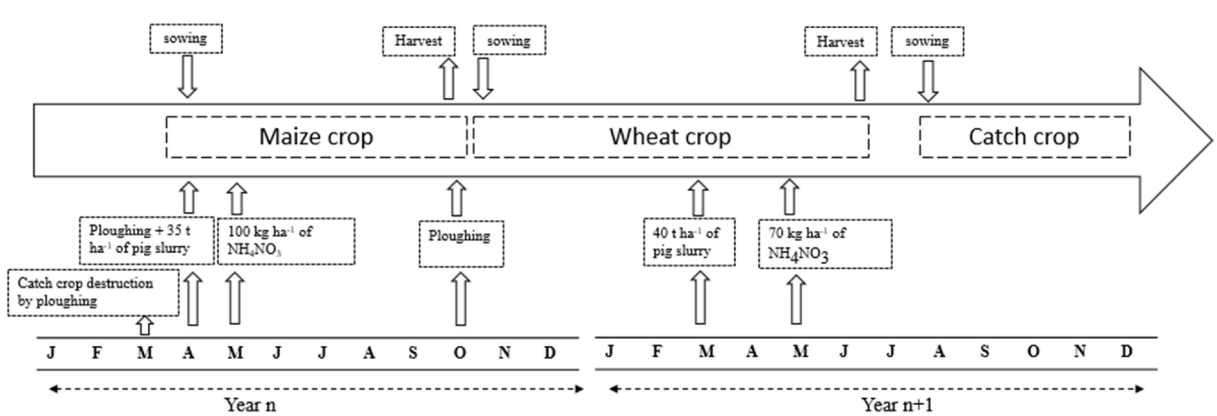

Fig. 3. The crop rotation simulated over the baseline period (maize-wheat-catch crop).

content of soil layers, available water, N mineralisation, N transfer, and water and carbon dynamics. Of these, nine daily outputs were selected to calculate SES indicators: crop transpiration, crop yield, water drainage, N leaching, plant N needs, amount of N mineralised from humus, N mineralised from organic residues, amount of organic N added to soil, and amount of SOC in humified organic matter.

2.5. Assessment of SES indicators

Six SES were assessed: two regulation SES: climate regulation via carbon sequestration and water quality regulation, four provisioning SES: N to plant provision, water to plant provision, plant biomass provision and groundwater recharge. Furthermore, both inter-annual and overall SES variabilities were analyzed based on biophysical SES indicators. All indicators used to infer SES were chosen based on the available literature and do not consider the catch crop, which was completely incorporated in the soil.

We developed two equations for each SES indicator. The first calculated the SES for each calendar year, while the second was the mean of these annual values over the baseline period (1988–2018).

- *Climate regulation (CS)* was defined as the ability of soils to sequester organic carbon. To quantify CS, we used the annual change in SOC stock from 0 to 30 cm as the indicator (Eq. (1)):

$$CS_j = CStock_{i+1} - CStock_i \tag{1}$$

$$\overline{CS} = \frac{1}{n}\sum_{j=1}^{n} CS_j \tag{2}$$

where $CStock_i$ is SOC stock from 0 to 30 cm of year i and n is the number of years considered (n = 30, 1988–2018).

$\overline{CS}$ is the annual average of CS over the baseline period.

- *Water quality (WQ) regulation* describes the soil's ability to store N and decrease N leaching. It was calculated as a ratio of the mean annual amount of N not leached to the total amount of N in the soil and supplied by fertilisation (Eq. (3)):

$$WQ_j = \frac{1}{365}\sum_{i=1}^{365}(1 - N\ leaching_i/(Nmin_i + azomes_{(i-1)} + anit_i) \tag{3}$$

$$\overline{WQ} = \frac{1}{n}\sum_{j=1}^{n} WQ_j \tag{4}$$

where *i* and *j* are respectively, the day and year considered, $Nleaching_i$ is the amount of N leached daily from the soil, $Nmin_i$ is the amount of mineral N produced daily by mineralisation of soil organic matter, crop residues and organic fertilisers, $anit_i$ is the amount of fertiliser N added daily to the crop, and $azomes_{(i-1)}$ is the amount of N in the soil profile on day *i-1*.

$\overline{WQ}$ is the annual average of WQ_j indicator over the baseline period.

WQ_j ranges from 0 (poor water quality regulation service) to 1 (high water quality regulation service).

- *N to plant provision (NP)* describes the soil's ability to meet plant N needs during the crop rotation without any mineral fertilisation. We chose a normalised indicator that ranges from 0 to 1. First, we calculated the ratio of available mineralised N, which can be easily taken up by roots, to plant N needs from sowing to harvest. Based on STICS outputs, this SES indicator was calculated using Eq. (5):

$$NP_j = \frac{1}{365}\sum_{i=1}^{365} min(1, Nh_i + Nr_i + azomes^* - Nleaching_i/Nplant_i) \tag{5}$$

$$\overline{NP} = \frac{1}{n}\sum_{j=1}^{n} NP_j \tag{6}$$

where Nh_i is the amount of N mineralised daily from humus, Nr_i is the amount of N mineralised daily from organic residues (crop residues and organic fertilisers), azomes* is the amount of N in the soil profile on the sowing date of each year and N $plant_i$ is daily plant N needs.

$\overline{NP}$ is the annual average of NP_j over the baseline period.

The ratio equals 1 if all plant needs are met, exceeds 1 if available N exceeds plant needs and is less than one if available N is insufficient. NP equals the ratio limited to a maximum value of 1; thus, excess N available for plants was not considered. Also, as the catch crop was completely returned to the soil and not exported, it was not considered in SES assessment.

- *Water to plant provision (WP)* describes the soil's ability to store and provide water to plants without irrigation. It depends strongly on available water capacity, rainfall pattern and crop phenological stage. We adopted EFESE-EA (2017)'s indicator: mean annual recovery rate of water plant needs during the crop rotation. Consequently, we used plant transpiration rates over the rotation of spring and winter crops (Eq. (7)):

$$WP_j = \sum_{i=sowing\ date\ crop\ 1}^{harvest\ date\ crop\ 1} ep_i + \sum_{k=sowing\ date\ crop2}^{end\ of\ calendar\ year=365} ep_k \tag{7}$$

$$\overline{WP} = \frac{1}{n}\sum_{j=1}^{n} WP_j \tag{8}$$

where ep_i is daily crop1 (maize) transpiration and ep_k is daily crop2 (wheat) transpiration.

$\overline{WP}$ is the annual average of WP_j over the baseline period.

- *Plant biomass provision (YE)* describes the soil's ability to produce plant biomass by photosynthesis. It represents the annual yield of cash crops and expressed in energy units (kcal ha^{-1} $year^{-1}$). Hence, like WP and NP, YE was calculated by excluding the catch crop. We converted dry matter yields of maize and wheat into energy according to FAO specifications (FAO, 2003) using Eq. (9):

$$YE_j = \frac{1}{n}\sum_{i=1}^{n} B_i{}^*k \tag{9}$$

$$\overline{YE} = \frac{1}{n}\sum_{j=1}^{n} YE_j \tag{10}$$

where B_i is the dry matter of harvested biomass and *k* is a conversion coefficient to express biomass in terms of energy (3.34 kcal g^{-1} for maize and 3.19 kcal g^{-1} for wheat).

$\overline{YE}$ is the annual average of YE_j over the baseline period.

Groundwater recharge (GW) describes the soil's ability to recharge groundwater. It considers water that infiltrates into the soil and percolates into the groundwater. GW is calculated as the sum of daily water drainage from the soil, which is assumed to reach the groundwater, over one calendar year (Eq. (11)):

$$GW_j = \sum_{i=1}^{365} D_i \tag{11}$$

$$\overline{GW} = \frac{1}{n}\sum_{j=1}^{n} GW_j \tag{12}$$

where Di is the amount of water drained daily from the soil (mm).

$\overline{GW}$is the annual average of GW_j over the baseline period.

2.6. Statistical analysis

Simulation outputs characterised spatio-temporal variability in SES indicators at 64 sites that covered the primary variability of the study area. To analyse inter-annual variability in SES, SES relationships and the soil properties that influenced them, several statistical analyses were performed.

First, we calculated coefficients of variation (CV) of the inter-annual SES values to compare distributions of SES with different units. It measures the variability of each indicator by dividing its mean value by its standard deviation. Formally, it is calculated using Eq. (13), in which M and S are the mean and standard deviation of each SES indicator over the baseline period, respectively.

$$CV = M \times 100/S \tag{13}$$

Second, we used a bagplot representation to visualise the relationship between each pair of SES indicators. The bagplot is a generation of the univariate boxplot (Tukey, 1975) to bivariate data. It depicts the location (position of median depth), spread (bag area), correlation skewness (bag shape) and outliers of the dataset (Rousseeuw et al., 1999). We generated bagplots using the bagplot function of the aplpack package of R software (R Core Team, 2019).

Third, we calculated a Pearson correlation matrix between each pair of mean SES indicators and soil determinants to demonstrate the degree of interactions among variables and select those exerting the major influence. To visualize the correlation matrix, we generated a network chart using the qgraph package of R software. To remove edges that were not significant, we used the Bonferroni threshold (Curtin and Schulz, 1998).

Fourth, we performed a normalised PCA to assess gradients that separated sites according to SES indicator means and their associated standard deviations over the baseline period. Continuous soil properties such as SOC content, available water capacity, maximum rooting depth, soil pH and clay content were used as supplemental variables. These soil properties were selected because they are the ones used most frequently in SES studies, as reported by Greiner et al. (2017) and Dominati et al. (2014).

Fifth, to identify linear relationships between each SES metric and soil properties, stepwise multiple-linear regression was performed. We used the Akaike Information Criterion (AICc) to select the best models. The statistical significance of model parameters was estimated by analysis of deviance (validated by F tests) between a null model (no effect) and a model that included one or more explanatory variables. Statistics were calculated and graphical outputs were generated using the ade4 package (Dray and Dufour, 2007) of R software.

Finally, we performed multivariate analysis of variance (MANOVA) to test differences in means of SES indicators between two or more groups of soil properties. The resulting variances were similarly tested against F statistics approximated by Wilks' lambda. For the MANOVA, we transformed continuous soil properties into categorical properties. We defined two classes for pH (<6, >6), three classes for clay content (<20%, 20–30%, >30%), two classes for soil depth (shallow (<60 cm) and deep (>60 cm)) and three classes for soil drainage (well drained, moderately drained and poorly drained) according to Vincent et al (2018). Finally, based on field pedological description of soil profiles, we defined 10 classes for parent materials and seven for soil types (succession of diagnostic or pedogenetic horizons).

3. Results

3.1. Inter-annual means of SES over the study area

All SES indicator means over the study area varied greatly, except for NP (Table 2). For instance, YE varied from 1 to 3 10^7 kcal ha^{-1} year^{-1}, WP varied from 110.4 to 286.9 mm year^{-1} (median = 192.6 mm year^{-1}) and GW varied from 103.3 to 282.5 mm year^{-1} (median = 186.4 mm year^{-1}). For regulation SES, mean WQ was high and ranged from 0.69 to 0.99. CS varied more, from −773.7 to 914.7 kg ha^{-1} year^{-1}. In contrast, NP varied little, ranging from 0.84 to 1.00 (median = 0.99).

Table 2
Descriptive statistics of mean values of soil ecosystem services (SES) over the baseline period estimated at the 64 sites (WP: water to plant provision; YE: Plant biomass provision; CS climate regulation; WQ: water quality regulation; GW: groundwater recharge; NP: N to plant provision).

SES	Min	Median	Mean	Max
WP (mm year^{-1})	110.4	192.6	193.6	286.9
GW (mm year^{-1})	103.3	186.4	182.5	282.5
NP	0.84	0.99	0.98	1.00
YE 10^7 (kcal ha^{-1}year^{-1})	1.00	1.85	1.96	3.03
CS (kg ha^{-1} year^{-1})	−773.7	139.5	126.5	914.7
WQ	0.69	0.86	0.86	0.99

3.2. Inter-annual temporal variability in SES indicators

As an example, in two soils with contrasting characteristics – shallow and sandy (Leptosol) vs. deep and loamy (Endostagnic Cambisol) – inter-annual variability (CVs) in SES was high: 17–36% and 7–65%, respectively (Fig. 4). Over the baseline period, wheat and maize yields were nearly twice as high for the deep loamy soil as those for the shallow sandy soil. Moreover, YE was relatively constant over time for the shallow soil regardless of the crop (0.9–1.5 10^7 kcal ha^{-1} year^{-1}). In contrast, YE for the deep soil had more inter-annual variability for maize (1.7–4.2 10^7 kcal ha^{-1} year^{-1}) than for wheat.

WP was highest for the deep loamy soil, exceeding 300 mm year^{-1} in 1993, 1997, 2007 and 2015, but did not exceed 200 mm year^{-1} for the shallow soil in the same years. As the winter and spring crops had similar trends in WP for both soils, we can conclude that both crops had similar water needs over their phenological stages. In contrast, GW was highest for the shallow sandy soil (>400 mm year^{-1} in 1999) but lowest for the deep loamy soil (<50 mm year^{-1}). Furthermore, GW for both soils displayed cyclical and unstable behavior that was lower and less variable for wheat over the baseline period.

NP usually remained high over the study period for the deep loamy soil, varying from 0.7 to 1.0 for maize and reaching its maximum value (1.0) for wheat. In contrast, NP for the shallow soil had high inter-annual variability, varying from 0.38 to 1.0 for maize and 0.5–1.0 for wheat.

For regulation SES, both soils had high WQ, which usually ranged from 0.8 to 1.0 for the deep loamy soil. For instance, it reached its maximum value (1.0) in 1988, 1999, 2004 and 2017 and was nearly 0.9 in 1990, 1994, 1999, 2008 and 2018, meaning that at least 10% of the N provided was leached from the soil. However, the shallow soil had large inter-annual variability over the baseline period, ranging from 0.4 to 0.9. Interestingly, for the deep loamy soil, WQ was similar for both crops over time. In contrast, WQ dynamics for the shallow sandy soil were similar to those for the deep loamy soil for wheat but differed greatly for maize.

Finally, CS was higher for the shallow soil than for the deep soil, regardless of the crop. For the shallow soil, carbon sequestration was predicted for all years, except for wheat in 2014 and 2018, when CO_2 losses reached nearly 180 kg ha^{-1} year^{-1}. Meanwhile, CS for the deep loamy soil was marked over the baseline period by an alternating cycle of years of net soil carbon storage and loss. The wettest years, particularly 1997, 2000, 2014 and 2015, with total rainfall >800 mm year^{-1}, had high CO_2 losses.

3.3. Spatial variability of the average estimates of SES indicators over the baseline period (30 years)

Although cropping practices and weather data were the same, each SES indicator varied greatly among soil types (Fig. 5). For instance, YE differed greatly among soils. Mean (±1 standard deviation) YE (maize

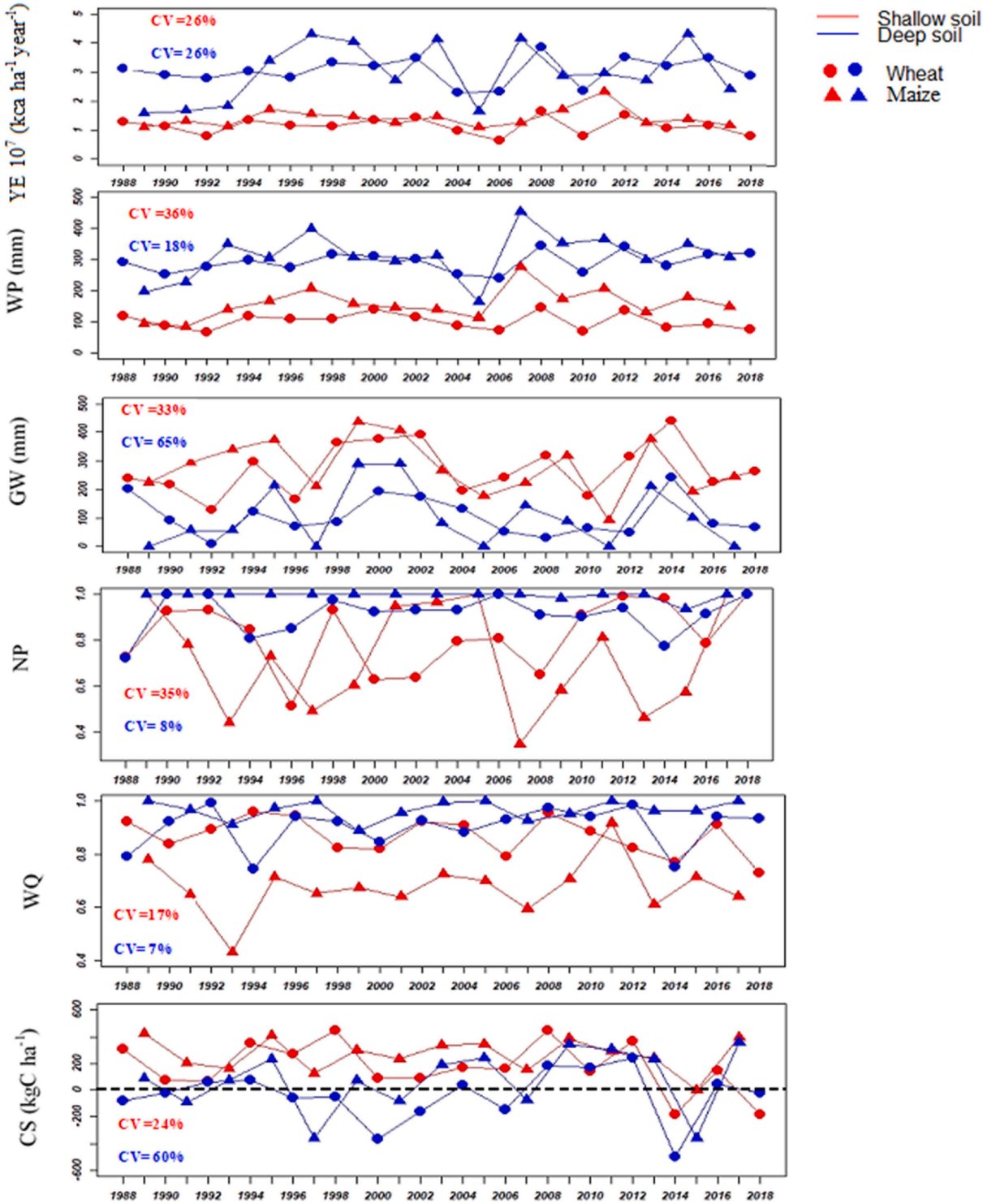

Fig. 4. Annual soil ecosystem service values for maize and wheat crops for two contrasting soils over the baseline period (red: coarse-textured Leptosol overlying gritty schist with a depth of 30 cm (Table 1; N86b); blue: Endostagnic Cambisol on deep loam with a depth of 150 cm (Table 1: L61a).

and wheat combined) reached 2.63 ± 0.60 10^7 kcal ha^{-1} $year^{-1}$ (Table 3) for a Luvisol developed on loess soil (L4C1) but did not exceed 1.40 ± 0.36 10^7 kcal ha^{-1} $year^{-1}$ (Table 3) for a sandy Leptosol (L4C1). Likewise, WP was higher for fine-textured soils (289 ± 56 mm $year^{-1}$ for R17b) but lowest for coarse-textured soils (130 ± 48 mm $year^{-1}$ for R0R5).

GW was low (122 ± 88 mm $year^{1}$) for a Luvisol (L0C1) in a lowland with high available water storage capacity (200 mm for a depth of 100 cm) (Table 3). GW reached 283 ± 90 mm $year^{-1}$ for a Leptosol (R0R5) with a low available water storage capacity (<36 mm) (Table 3). Overall, GW depended strongly on soil depth and thus on available water storage capacity. It was high for shallow sandy soils and low for deeper loamy soils.

Mean NP values were high, ranging from 0.75 (T8a) to 1.0 (Vm8Th1) (Table 3), indicating that at least 75% of plant N needs were covered. As the same amount of fertiliser was applied each year over the baseline

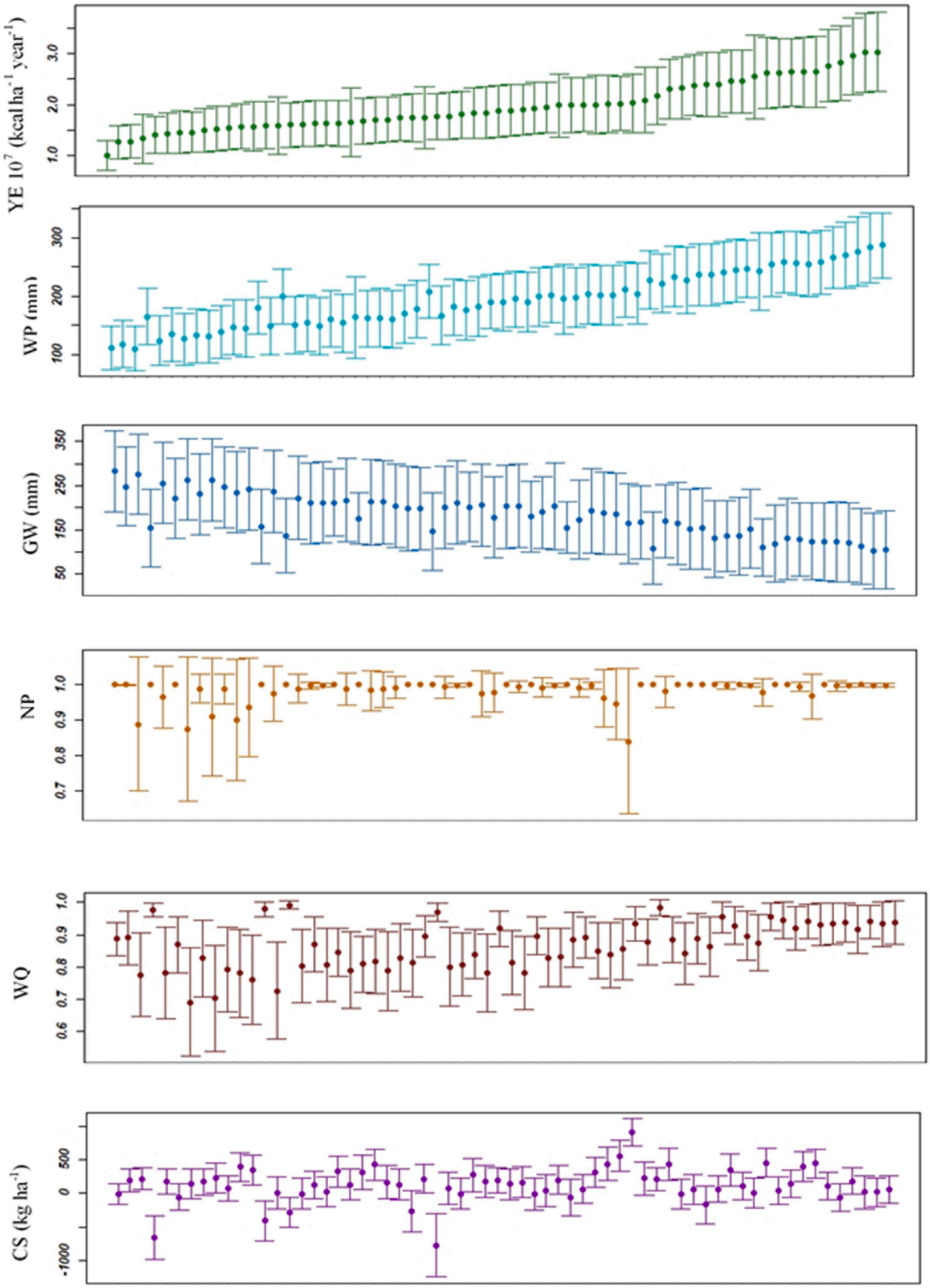

Fig. 5. Mean soil ecosystem service indicators of the 64 sites studied, ranked by increasing plant biomass provision (YE). Error bars represent the standard deviation.

Table 3
Mean (and standard deviation) of soil ecosystem service values over the baseline period (30 years) for 16 representative sites. These sites were selected by ranking the 64 sites by increasing yield then retaining every fourth site (WP: water to plant provision; YE: Plant biomass provision; CS climate regulation; WQ: water quality regulation; GW: groundwater recharge; NP: N to plant provision).

Soil-code	WP (mm)	GW (mm)	NP	YE (10^7 kcal)	CS (kg ha^{-1})	WQ
R0R5	130	283	0.99	1 (0.3)	−7.76	0.88
	(48)	(90)	(0.05)		(150)	(0.05)
N0R5	142	256	0.84	1.4	187	0.78
	(48)	(91)	(0.24)	(0.36)	(188)	(0.14)
T0B5	150	263	0.75	1.5	232	0.70
	(54)	(93)	(0.27)	(0.42)	(219)	(0.16)
Vm8Th1	199	158	1(0)	1.57	−406	0.98
	(52)	(84)		(0.48)	(299)	(0.02)
T4B4	172	210	0.91	1.62	126	0.87
	(55)	(93)	(0.13)	(0.42)	(206)	(0.08)
R5B3	182	176	0.97	1.65	318	0.80
	(84)	(58)	(0.06)	(0.66)	(262)	(0.08)
V5V4	187	298	0.96	1.74	−267	0.81
	(56)	(94)	(0.07)	(0.45)	(307)	(0.10)
N0B3	200	212	0.92	1.77	2.67	0.80
	(56)	(95)	(0.12)	(0.45)	(229)	(0.0)
U5C1	208	203	0.93	1.87	142	0.81
	(55)	(94)	(0.11)	(0.05)	(234)	(0.09)
L1C1	221	203	0.97	1.95	203	0.83
	(50)	(98)	(0.05)	(0.48)	(211)	(0.09)
T3B3	220	187	0.86	2 (0.56)	443	0.83
	(58)	(93)	(0.18)		(211)	(0.10)
Vm3Th1	247	109	0.96	2.1 (0.6)	213	0.98
	(55)	(82)	(0.07)		(178)	(0.02)
Vm0Th1	254	154	0.98	2.38	−170	0.86
	(56)	(89)	(0.05)	(0.61)	(222)	(0.08)
Vm0Th1	264	152	0.97	2.45	1.42	0.87
	(56)	(91)	(0.04)	(0.58)	(278)	(0.09)
L4C1	275	127	0.92	2.63	402	0.94
	(56)	(83)	(0.1)	(0.6)	(225)	(0.05)
L0C1	289	122	0.93	2.81	186	0.91
	(56)	(88)	(0.1)	(0.7)	(202)	(0.07)

period, NP was usually high regardless of the soil type. In general, no N stress was predicted during the phenological crop stages, and all crop N needs were satisfied by mineralisation of crop residues. More importantly, only deep soils had the highest NP (1.0). Shallow soils had lower NP.

Mean WQ was high, even though the rotation had a constant annual N supply. WQ ranged from 0.70 ± 0.16 (T0B5) to 0.98 ± 0.02 (Vm3Th1, Table 3). Furthermore, WQ differed significantly among soil types, being highest for deep soils with a fine texture, such as an Endostagnic Cambisol with a loamy texture (L4C1: 0.94 ± 0.05, Table 3). In contrast, WQ was relatively low for shallow soils, such as a Leptosol developed on granite with a coarse texture (T0B5: 0.70 ± 0.16, Table 3). Overall, WQ had the lowest mean values for fine-textured soils in depressions and the highest mean values for coarse-textured soils on coastal plains and for soils rich in organic matter.

For CS, situations of carbon storage or loss were identified. As soils were ploughed twice per year to a depth of 25 cm, both deep and shallow soils had negative carbon balances. For 21% of the sties, mean annual loss rate varied from nearly −773 to −3 kg ha^{-1} (Fig. 5). In general, negative balance was due to mineralisation, which released SOC as CO_2 into the atmosphere. In comparison, 79% of the sites had positive carbon balances, with mean annual increase of 1.42–914 kg ha^{-1} (Fig. 5). Interestingly, shallow soils had higher mean CS than deep soils.

Overall, except for NP, all SES indicators varied greatly among sites and reached their maximum value at least once. More importantly, soils with the highest YE had the highest WP, lowest GW, maximum NP (1.0) and highest WQ. In addition, except for CS, the standard deviation of all SES varied greatly among sites. Hence, soil diversity in the landscape, which is related to the nature of the geological substrate and other pedological factors, was the main driver of SES provision.

3.4. Interrelation between SES

Most bagplots of each pair of SES indicators means for the 64 sites over 30 years had roughly the same area, so their associated values had a similar spread (Fig. 6). However, the bags had different orientations: some sloped upward (positive correlation) (YE-WP, Fig. 6a; WQ-WP, Fig. 6f), whereas others sloped downward (GW-YE, Fig. 6b). All bagplots were relatively circular and slightly skewed because their medians lay near the center of each bag. Finally, all datasets were medium-tailed based on the size of the "loop" (the boundary separating inliers from outliers) and the absence of outliers.

Overall, linear correlations produced results similar to those revealed by the bagplots. WP had the highest positive correlation, with YE (r = 0.97), followed by WQ (r = 0.66), and the highest negative correlation, with GW (r = −0.93) (Table 4). YE had a high negative correlation with GW (r = −0.86) and a high positive correlation with WQ (r = 0.52). Overall, the correlation matrix highlighted significant correlations between all SES, except for NP and CS, which were negative (r = −0.48). The network chart of the SES highlighted the main relationships between them (Fig. 7). Overall, YE was strongly synergic with WP and WQ but showed a trade-off with GW. Likewise, WQ had strong synergies with WP and NP. Significant trade-offs were observed among many pairs of SES, such as GW and WP, GW and WQ, CS and NP, and NP and GW.

3.5. Interrelation between SES and soil properties

In general, WP was strongly and positively correlated with some soil properties, such as available water capacity (r = 0.98) and maximum rooting depth (r = 0.86) (Table 4). Similarly, YE had high positive correlation with available water storage capacity (r = 0.92) and maximum rooting depth (r = 0.73) and significant negative correlation with clay content (r = −0.47) and SOC content (r = −0.45). On the other side, CS was strongly correlated only with physicochemical soil properties such as SOC content (r = −0.66), pH (−0.71) and clay content (r = −0.51). Visual inspection of this correlation network chart (Fig. 8) highlighted the predominant role of soil depth via maximum rooting depth and available water storage capacity. These variables were strongly correlated with WP, YE, WQ and GW. More importantly, GW was negatively correlated with WP, WQ, YE (Fig. 7) and soil depth variables (Fig. 8). In contrast, NP and CS were correlated only with physicochemical soil properties. Thus, soil depth and soil hydrological features were the main drivers of GW, WQ, WP and YE, whereas physicochemical soil properties were the main drivers of NP and CS. These relationships were mainly driven by the STICS model assumptions.

3.6. Multivariate analysis of interrelations between SES and soil properties

Projecting all variables onto the PCA factorial plan, the first two PCs explained nearly 70% of the total variance, of which PC1 explained 50.5% (Fig. 9a). PC1 contrasted YE, WP, WQ and GW, whereas PC2 contrasted CS and NP. More importantly, WP and GW were positively correlated with their standard deviations, whereas NP, CS and WQ were negatively correlated with their standard deviations. Projection of supplemental soil properties on PC1 highlighted that water holding capacity and soil depth were strongly correlated with YE, WP and GW. Furthermore, pH, clay content and SOC content were strongly correlated with NP and CS. Thus, depth and texture soil characteristics influenced water-related SES, while physicochemical soil properties influenced carbon and N balances.

By adding barycenter ellipses (α = 5%) of parent material and soil type groups to the PCA results, we distinguished seven ellipses for parent material (Fig. 9b) and four ellipses for soil type (Fig. 9c). Overall, the PCA accurately separated the sites according to their soil type, particularly Histosols, Luvisols, Cambisols and Leptosols. Luvisols were associated with high YE and WP. Histosols were associated with high WQ

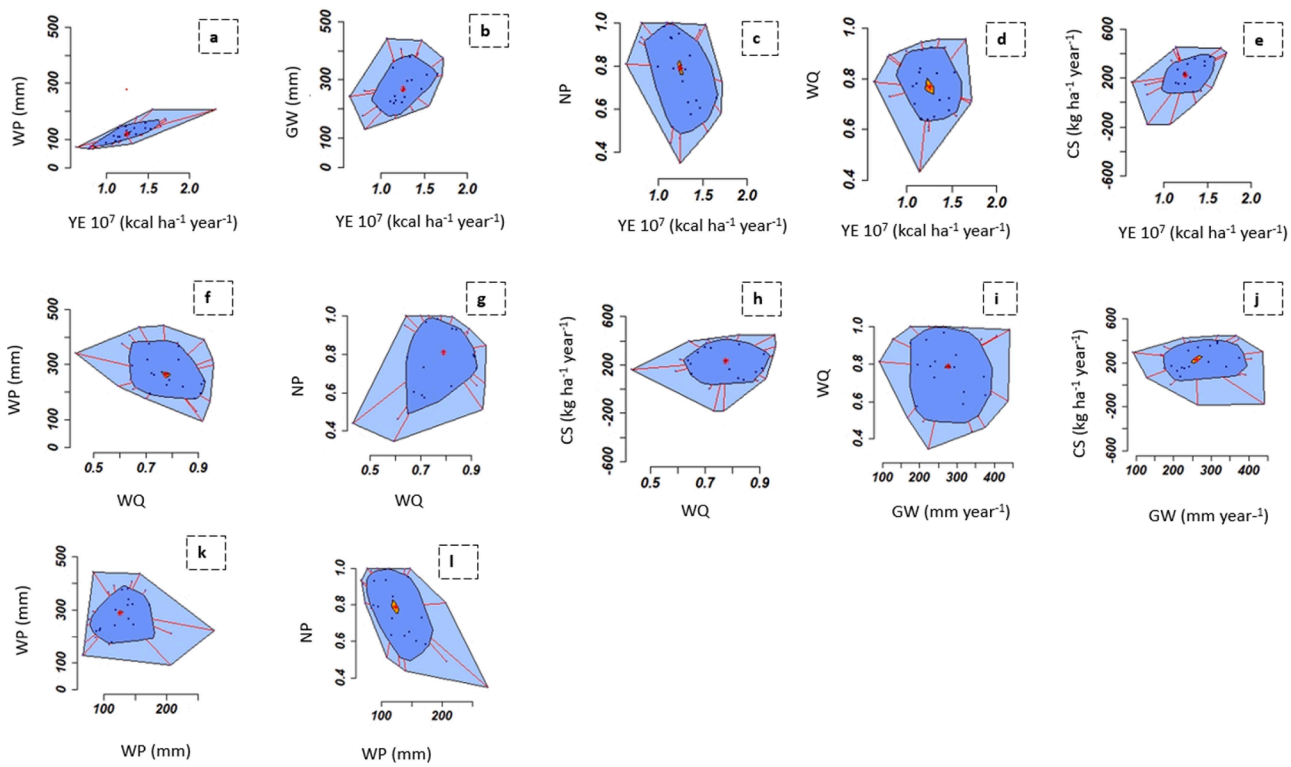

Fig. 6. Bagplots of pairs of soil ecosystem service indicators. Darker shading identifies the bag that contains 50% of observations, while lighter colored shading identifies the boundary separating inliers from outliers (the "loop"). Asterisks identify the point with highest half space depth (median depth) with its 95% confidence region.

Table 4
Pearson correlation coefficients (r) between soil ecosystem service (SES) indicators and soil properties. (WP: water to plant provision; YE: Plant biomass provision; CS climate regulation; WQ: water quality regulation; GW: groundwater recharge; NP: N to plant provision; AW: available water capacity; Obs: maximum rooting depth; pH: soil pH of the topsoil; CC: carbon content of the topsoil; Cly: clay content of the topsoil)

SES	WP	GW	NP	YE	CS	WQ	AW	Cly	pH	CC
WP	1									
GW	−0.93***	1								
NP	0.31	−0.39	1							
YE	0.97***	−0.86***	0.25	1						
CS	0.02	0.11	−0.48**	0.13	1					
WQ	0.66***	−0.81***	0.4	0.52***	−0.23	1				
AW	0.98***	−0.94***	0.33	0.92***	−0.04	0.73***	1			
Cly	0.31	0.03	0.18	−0.47***	−0.51**	0.37	−0.17	1		
pH	0.27	−0.35	0.55**	0.17	−0.71***	0.37	0.34	0.42*	1	
CC	0.33	0.16	0.05	−0.45*	−0.66***	0.23	−0.26	0.61***	0.1	1
Obs	0.86***	−0.85***	0.38	0.73***	−0.16	0.68***	0.88***	−0.01	0.1	−0.12

Asterisks denote significance (*t*-test) (* $P < 0.05$; ** $P < 0.01$; *** $P < 0.001$);

and NP. Cambisols had high CS, while Leptosols had the highest GW.

Regarding parent material, clusters of alluvial terrace, gritty schist, sandstone and granite overlapped substantially, whereas those of loess and marsh were widely separated. Loess parent material was associated with YE and WP, marsh was associated with NP and WQ, and the other clusters were associated with CS and GW. Hence, shallow sandy soils had the highest GW and CS, deep loamy soils with high soil water storage capacity had the highest YE and WP and the relatively hydromorphic Histosols had the highest WQ and NP.

Stepwise multiple–linear regression for each of the six SES indicators highlighted the large contribution of inherent and manageable soil properties to explaining the indicators. In general, all SES regression equations had high adjusted R^2 values (>0.80), except for NP, for which it was low (0.30) (Table 5). All SES indicator regressions were significant at $p < 0.001$.

As expected, variability in SES indicators was driven mainly by soil characteristics. The MANOVA (Table 6) demonstrated that SES provision differed significantly between the three classes of clay content, the two classes of soil pH, the two classes of soil depth, the three classes of soil drainage, the 10 classes of soil parent material and the seven classes of soil type. Therefore, SES provision differed for each soil property class, and the pure effect of soil determinants was significant regardless of the SES.

4. Discussion

4.1. Comparing SES evaluations with a focus on the modelling approach limitations

Six SES indicators were estimated using the STICS model, and then interrelations between SES and between SES and soil properties were investigated. This study contributes to an emerging literature that

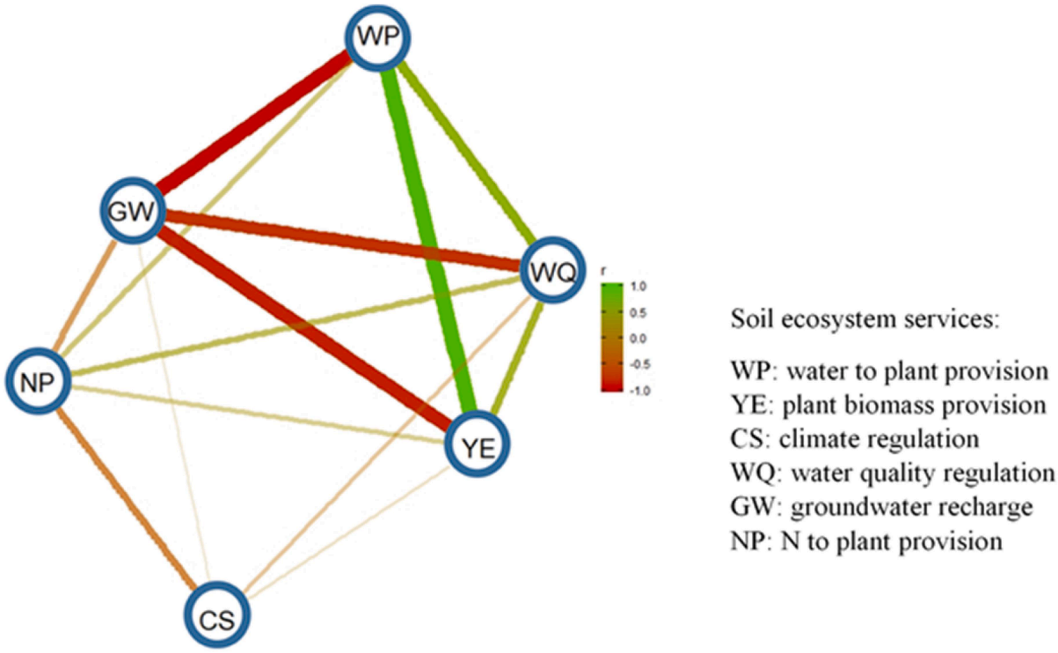

Fig. 7. Correlation network chart showing interrelations among soil ecosystem service indicators based on their mean values over the baseline period. Only significant correlations are shown. Line width indicates correlation intensity.

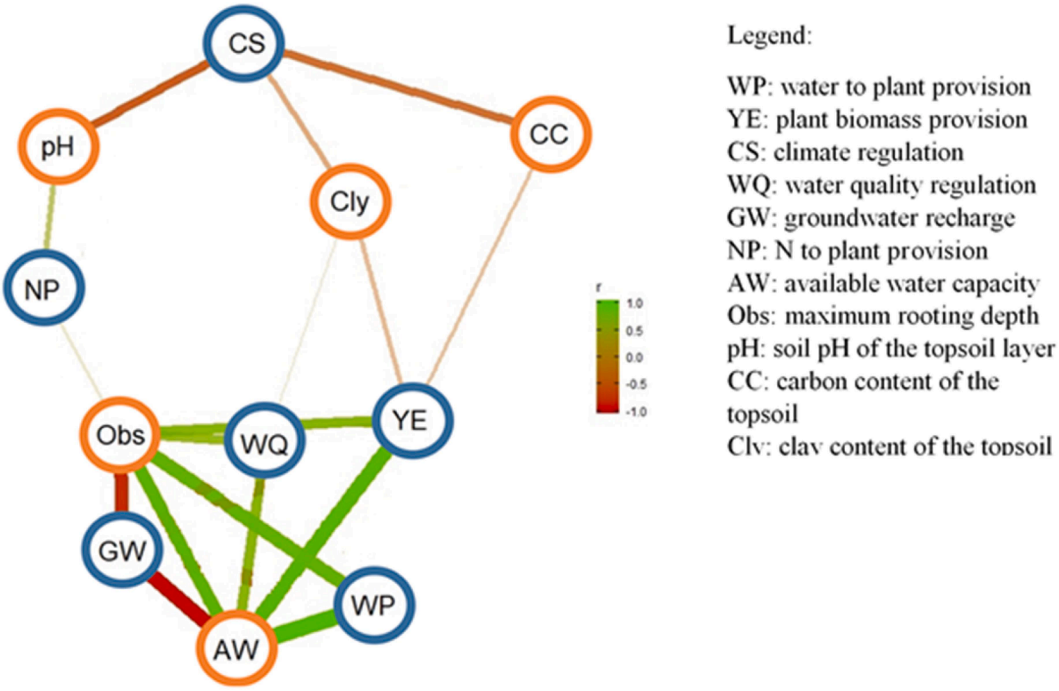

Fig. 8. Network chart showing interrelations between the SES indicator means values over the baseline period (blue circles) and soil properties (orange circles). Only significant correlations are shown. Line width indicates correlation coefficient intensity.

attempts to assess multiple SES and their interrelations at a large scale. Analysing how SES provision varies with pedological variability over a long temporal scale distinguishes our approach from other studies, such as those of Calzolari et al. (2016) and Grimaldi et al. (2014). These studies considered SES as static and assessed them using a set of indicators expressed at a given point in time.

As mentioned by Beaudoin et al. (2008), STICS simulates crop production without any significant temporal drift. For instance, the mean yield of winter wheat among the 64 sites was predicted at 7.6 and 6.3 t ha^{-1} in 2014 and 2018, respectively, similar to those reported in agriculture surveys in the Agreste database for the Ille-et-Vilaine department (7.5 and 6.8 t ha^{-1}, respectively). Likewise, the mean yield of grain maize was predicted at 8.4 and 8.6 t ha^{-1} in 2015 and 2017, respectively, similar to those in the Agreste database (ca. 8.5 q ha^{-1} in both years). Even though STICS does not consider many factors, such as pests and diseases, it predicted biomass production over the baseline period well. When present, these factors can reduce crop production greatly (Meynard et al., 2002; Beaudoin et al., 2008; Fraga et al., 2018).

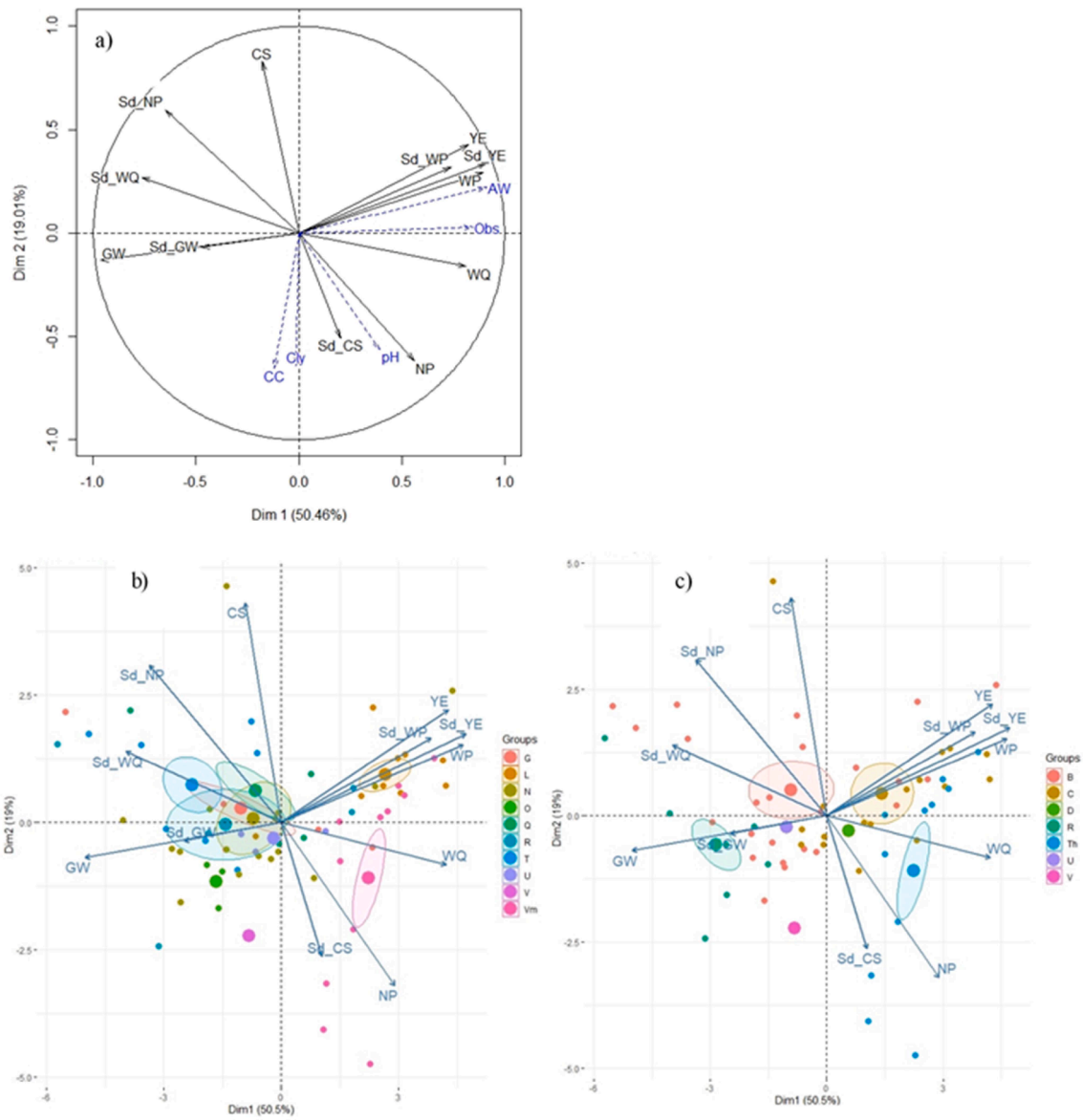

Fig. 9. a) Plots of SES indicator means with their associated standard deviations and some soil properties as supplemental variables on the two first PCA principal components. b) Biplot of PCA variables and the 64 sites according to parent material (α = 5%) (G: granite, L: loess, N: soft schist, O: medium schist, R: gritty schist, T: alluvial terrace, U: colluvial deposits, V: alluvial deposits, Vm: marsh) c) Biplot of PCA variables and the 64 sites according to soil type (α = 5%) (B: Cambisol, C: Endostagnic Cambisol, D: Stagnic Alluvisol, R: Leptosol, Th: Histosol, U: Colluvic Cambisol, V: Fluvisol).

Table 5
Statistics of stepwise multiple linear regression models predicting means soil ecosystem service (SES) values over the baseline period as a function of soil properties. (WP: water to plant provision; YE: Plant biomass provision; CS climate regulation; WQ: water quality regulation; GW: groundwater recharge; NP: N to plant provision; AW: available water capacity; Obs: maximum rooting depth; pH: soil pH of the topsoil; CC: soil organic carbon content of the topsoil; Cly: clay content of the topsoil).

SES	Soil properties selected in the model	Adjusted R^2	F-statistic	Significance
WP	AW, clay, soil depth class	0.97	849	<0.001
GW	AW, clay, obs, soil drainage, soil depth class	0.91	119	<0.001
NP	pH	0.30	26	<0.001
YE	AW, clay, obs	0.94	362	<0.001
WQ	AW, pH, CC, clay, obs, soil depth class	0.82	49.6	<0.001
CS	pH, CC, clay, soil depth class	0.87	110	<0.001

Table 6
Results of a Multivariate Analysis of Variance (MANOVA) model comparing clay, soil pH, parent material, soil type, soil depth and soil drainage effects on mean values of soil ecosystem services over the baseline period. The F-statistic, approximated from Wilks' lambda, denotes the importance of model terms in explaining SES.

Term	F-statistic	Significance
Clay	0.22	<0.001
Soil pH	0.57	<0.001
Parent material	0.08	<0.001
Soil type	0.15	<0.001
Soil depth	0.52	<0.001
Soil drainage	0.26	<0.001

Our results showed that GW depended strongly on soil depth and available water storage capacity. Shallow soils with coarse texture had the highest GW, whereas deep soils with a medium texture had the

lowest GW. GW was estimated at 298 (±94) or 122 (±88) mm for soils with a water storage capacity < 40 mm or 120 mm, respectively (Table 3) The EFESE-EA (2017) study also demonstrated this trend, highlighting that GW increased as water storage capacity decreased, and vice versa. In their study, GW reached 430 mm and did not exceed a mean of 300 mm for soils with a water storage capacity <40 or >120 mm, respectively. The difference in GW reported by these studies may have several explanations. First, EFESE-EA STICS simulations were based on pedoclimatic units whose soil features were available at 1:1.000,000 scale. Hence, the relative accuracy of soil data, particularly those of stony materials, can influence GW predictions significantly. Second, hydrodynamic soil properties such as W_{FC}, W_{WP} and bulk density were estimated using different regional and national pedotransfer soil functions. Finally, EFESE-EA predictions were based on a hydrological year time step (1 September to 31 August), whereas our predictions were based on a calendar-year time step (1 January to 31 December). In addition, some limitations of STICS should be noted. STICS is a field-scale model that simulates only water flows at a single point, rather than within an area. Therefore, it does not consider lateral spatial interactions, though it can consider deep percolation.

WP was directly proportional to water storage capacity. Indeed, mean WP was ca. 130 mm year^{-1} for shallow sandy soils but >200 mm year^{-1} for deep loamy soils. This result agrees with those of the EFESE-EA, which reported similar WPs strongly correlated with water storage capacity. In general, both soil texture and structure influence pore-size distribution: medium- and fine-textured soils have high total water storage capacity due to high porosity and the ideal combination of meso- and micro-porosity (O'Geen, 2012). Likewise, Calzolari et al. (2016) demonstrated that fine-textured soils had a high-water storage capacity, whereas coarse-textured soils had a low water storage capacity.

As WQ is an N-based indicator, WQ and NP had similar responses to pedological variability. Both indicators exceeded a mean of 70%. They had high variability for shallow soils (low YE and high GW) and low variability for deep soils (high YE and low GW). This behaviour was related strongly to inherent soil properties (e.g. soil texture, soil depth), agricultural practices (e.g. mineral fertilisation, soil tillage) and rainfall pattern. Due to their large pore space, deep soils with less sand and more silt, clay or organic matter retained more N, which corroborates results of Powell-Graines and Gaines (1994), who studied the relationship between soil texture and N leaching. Furthermore, fine-textured soils can retain more N than coarse-textured soils, which directly influences N availability for plants: more N is available for plants in deep fine-textured soils than in shallow coarse-textured soils. Our results agreed those of the EFESE-EA (2017), which highlighted high N retention capacity of soils in Brittany. Furthermore, Van Wijnen et al. (2012) assessed natural decrease in pollutants using indicators of N-related processes (e.g. soil pH, potential mineralization rate of organic N, potential carbon mineralization rate, functional microbial activity). They found that natural decrease in pollutants is high in arable fields on clay soils and low in most arable fields on sandy soils. The same trend was also confirmed by Calzolari et al. (2016) and Dominati et al. (2014). However, most studies like ours assess WQ as the amount of N released into groundwater after passing through the soil profile. In fact, soils also filter organic matter, phosphorus (P) and pathogens, which can differ in form, stability and solubility and thus in the probability that they will be retained or released. In our context, the agricultural practices used involve adding exogenous organic matter and mineral fertilization. Therefore, assessing WQ as a function of P and dissolved organic carbon (DOC) leaching would provide an informative three-dimensional indicator (N, P and DOC).

CS reflects carbon flows that influence SOC stock 0–30 cm. Processes involved in carbon balance include net primary production, incorporation of crop residues, organic matter decomposition, erosion and DOC leaching. The net balance among these processes determines whether a soil loses or accumulates carbon. CS is provided when soil carbon accumulates (positive carbon net balance), but loss of soil carbon is considered degradation (Dominati et al., 2014). In the present study, situations of carbon accumulation or loss were identified, but no trends were identified as a function of soil types. This can be explained mainly by the complexity of carbon sequestration; which STICS is not a very performant model to simulate the carbon dynamics like more specific model such as Roth C and Century models. Carbon can be sequestrated through temporal changes in land use and agricultural practices (Ellili et al., 2019).

4.2. Explaining and interpreting SES interrelations

According to Qin et al. (2015) and Vallet et al. (2018), few studies have attempted to assess SES interrelations. In general, trade-off, synergy and neutral interactions between SES depend strongly on agro-pedoclimatic conditions (Fu et al., 2015). Our results showed strong synergy for the pairs WQ-NP, WQ-WP, YE-WQ and YE-WP, which means that both SES decrease or increase together. As expected, YE is synergic with WP, which is consistent with the literature. Many researchers (e.g. Bennett and Harms, 2013) observed a positive correlation between crop yield and crop transpiration. Water is a transporting agent for all plant physiological processes, and any water deficit can impair plant metabolism and consequently decrease crop yield. It was not surprising to find synergy between WQ and NP. As NP is based on soil N mineralization, increasing N availability for plants can increase biomass production and thus plant N uptake, which reduces N leaching from the soil. Likewise, both water and N requirements increase when crop yield increases, which may explain the synergy between WP and NP. Calzolari et al. (2016) found a similar relationship between YE and WQ when assessing multiple indicators. Other studies, such as that of Jopke et al. (2015), found a trade-off between crop production and water quality regulation (r = −0.23) at the European scale, albeit without distinguishing crop areas from forest or grassland.

It is notable that the pairs CS-YE, CS-GW and CS-WQ had non-significant relationships (r values close to 0). Jopke et al. (2015) also studied multiple SES, observing a neutral relationship between crop production and carbon storage, with no significant correlation ($r = -0.06$). Egoh et al. (2002) reported a weak correlation between primary productivity and carbon storage ($r = -0.14$), carbon storage and water supply ($r = 0.08$) and carbon storage and soil water retention ($r = -0.17$). In contrast, Raudsepp-Hearne et al. (2010), found a strong trade-off between crop production and carbon sequestration ($r = --0.88$). The differences among results can be explained by the simulation model we used to quantify SES: the absence of model validation for this set of SES may limit the confidence with which we can assess SES interrelations (Bagstad et al., 2013; Nemec and Raudsepp-Hearne, 2013).

The pairs GW-WP, GW-WQ and GW-YE displayed trade-off relationships. Overall, a decrease in GW implied a decrease in the amount of N that can reach the groundwater and thus an increase in WQ. Hence, as in former studies (e.g., United Nations, 2015), we identified a trade-off between provisioning SES (GW) and regulation SES (WQ). However, the trade-off between GW and WP and between GW and YE may be explained by temporal and geographic scale effects. In our context, the spring crop (maize) had high water requirements, particularly during the flowering period, which coincided with moderate rainfall amounts. The winter crop did not have this problem. Hence, an important caveat to our analysis is that temporal correlation was not considered when interpreting SES interrelations. Many researchers have used the "change over time" approach (Tomscha and Gergel, 2016) or "correlation analysis between the amounts of changes in SES" (Qin et al., 2015, Zheng et al., 2014) to detect changes in SES relationships over time.

4.3. Explaining and interpreting interrelations between SES and soil properties

Clearly, soil properties have a strong influence on SES provision.

Globally, soils differ at regional scales (Ellili Bargaoui et al., 2019; Vincent et al., 2018) down to the local scale of soil catenas (Ellili Bargaoui et al., 2019), at which landscape ecology is studied most. We considered easily accessible inherent soil properties such as soil parent material, soil type, soil depth and maximum rooting depth, as well as other properties measured in the top soil layer, such as SOC content, texture and pH. The correlation network chart (Fig. 8) indicated that maximum rooting depth and soil water storage capacity, which integrates effects of soil texture, structure and depth, were the main drivers of YE, WP, GW and WQ. These results are consistent with the literature. Dominati et al. (2014) clearly stated that available water capacity is an essential determinant of food provision supported by natural capital stocks. The distribution of pore sizes influences the supply of gases and nutrients to plant roots. In addition, available water capacity is a key factor not only for plant development but also for flow regulation, because it influences draining of excess water. Dominati et al. (2014) also pointed out that filtering of nutrients or contaminants and groundwater recharge depend strongly on soil depth, texture and structure. Many researchers (Calzolari et al, 2016; Clech'h et al., 2016; Egoh et al, 2008; Grimaldi et al., 2014; Greiner et al., 2017, Drobnik et al., 2018) argue that inherent soil properties, particularly soil structure, available water capacity and depth are the main drivers of provision of YE, WP, GW and WQ.

In the present study, YE and carbon content had a negative correlation ($r = -0.47$). This is probably due to our soil dataset, which was sampled following a stratified random sampling design to capture soil spatial heterogeneity over of the Brittany region. We also found a negative correlation between CS and pH, which is a strong driver of soil microbial diversity and strongly influences the microbial carbon cycle. It can regulate processes that influence carbon dynamics, particularly mineralization, assimilation and accumulation of organic matter inputs by soil microbial communities. Many studies, such as that of Malik et al. (2018), identified that soil pH negatively influences SOC stock.

In contrast to the review of Singh et al. (2017), we found a negative correlation between CS and clay content. It is likely that soils with high SOC are already saturated and will stock less than low SOC soils. This is consistent with Chen et al. 2018 results', who demonstrated that French's croplands are largely unsaturated. Clay content and SOC are significantly positively correlated (0.61, Table 4), which can explain the negative correlation between clay and CS. In general, carbon mineralization is lower in fine-textured soils than in coarse-textured soils (Hassink, 1992). As SOC is less accessible in fine-textured soils, the latter have a greater ability to protect SOC against microbial attack than coarse-textured soils (Hassink, 1997). However, carbon sequestration relies on complex interactions among soil properties, landscape management and environmental conditions that are complicated to simulate simultaneously.

As seen, the results of this study were generally similar to those of related studies. However, as correlation coefficients are the only measure available with which to compare results, we could not yet compare the additional information obtained with the PCA, MANOVA, regression-based methods or bagplots. More importantly, all statistical analyses were complementary and confirmed the strong influence of soil properties in explaining SES variances, which was consistent with Grimaldi et al. (2014)'s results. Surprisingly, for all SES except NP, >87% of the total variance of SES could be explained using only inherent soil properties. The MANOVA revealed that the bundle of SES differed significantly among soil-property groups ($p < 0.001$). The PCA, a co-inertia analysis, which is a more flexible multivariate method, confirmed that soil properties were the key drivers of SES provision and provided additional information about the relationships between SES and their associated standard deviations. Hence, as mentioned by Mouchet et al. (2014), PCA, bagplots, MANOVA, regression-based methods and correlation matrices are effective approaches to analyze SES interrelations, while network analysis is a powerful way to visualize their relationships. Although the present study attempted to capture temporal variability by averaging SES indicators over 30 years, it did not address the temporal dimension sufficiently.

5. Conclusion

We developed a methodological framework for assessing SES and analyzing interactions among them. We provided multiple SES indicators predicted by the STICS crop model, which used input data describing soils, weather and agricultural practices over 30 years. Our results showed that landscape-scale pedological variability, as well as within-soil variability, even though it was briefly investigated, were the key drivers of SES provision. We revealed that deep soil with good hydrodynamic properties produced the most biomass and satisfied plant water requirements the most due to its high-water holding capacity. In contrast, shallow soils with a coarse texture had the highest groundwater recharge but lower water-quality buffering. Most of our results were consistent with the literature, specifically with EFESE-EA (2017) results, regardless of the data used. In our context, YE-WP, YE-WQ and YE-NP displayed synergies, whereas GW-WQ, GW-WP and GW-YE displayed trade-offs. In the present study, we don't clearly demonstrate the typical tradeoff between provisioning services—i.e. production of agricultural goods such as (YE) and regulating services particularly carbon sequestration CS. This possibly due to the scale effect and the complexity of the carbon sequestration process. Overall, the spatial pattern of SES provision and interactions among SES should be studied in the future to provide maps for decision support for both stakeholders and decision makers.

CRediT authorship contribution statement

Yosra Ellili-Bargaoui: Conceptualization, Data curation, Formal analysis, Funding acquisition, Investigation, Methodology, Project administration, Resources, Software, Supervision, Validation, Visualization, Writing - original draft, Writing - review & editing. **Christian Walter:** Conceptualization, Data curation, Formal analysis, Funding acquisition, Investigation, Methodology, Project administration, Resources, Supervision, Validation, Visualization, Writing - review & editing. **Blandine Lemercier:** Conceptualization, Data curation, Formal analysis, Funding acquisition, Investigation, Methodology, Project administration, Resources, Supervision, Validation, Visualization, Writing - review & editing. **Didier Michot:** Conceptualization, Data curation, Formal analysis, Funding acquisition, Investigation, Methodology, Project administration, Resources, Supervision, Validation, Visualization, Writing - review & editing.

Declaration of Competing Interest

The authors declare that they have no known competing financial interests or personal relationships that could have appeared to influence the work reported in this paper.

Acknowledgements

The authors gratefully acknowledge all farmers from the Ille-et-Vilaine department involved in our research. We thank technical staff who actively participated in field sampling and laboratory analysis. This research was performed in the framework of the INRA "Ecoserv" metaprogram. This work was also funded by the Soilserv program funded by ANR (Agence Nationale de la Recherche) (ANR-16-CE32-0005-01).

Appendix A. Supplementary data

Supplementary data to this article can be found online at https://doi.org/10.1016/j.ecolind.2020.107211.

References

Adhikari, K., Hartemink, A.E., 2016. Linking soils to ecosystem services — a global review. Geoderma 262, 101–111. https://doi.org/10.1016/j.geoderma.2015.08.009.

Bagstad, K.J., Semmens, D.J., Winthrop, R., 2013. Comparing approaches to spatially explicit ecosystem service modeling: a case study from the San Pedro River, Arizona. Ecosyst. Serv. 5, 40–50. https://doi.org/10.1016/j.ecoser.2013.07.007.

Baize, D., Girard, M.C., 2008. Référentiel pédologique 2008, Association française pour l'étude du sol. BRGM: Carte géologique de la Bretagne. Available at <http://sigesbre.brgm.fr/Histoire-geologique-de-la-Bretagne-59.html>.

Baveye, P.C., Baveye, J., Gowdy, J., 2016. Soil "Ecosystem" services and natural capital: critical appraisal of research on uncertain ground. Front. Environ. Sci. 4 https://doi.org/10.3389/fenvs.2016.00041.

Baumont R, Dulphy JP, Sauvant D, Tran G, Meschy F, Aufrère J, Peyraud JL, Champciaux P. Les tables de la valeur des aliments (Livre rouge). In : Alimentation des bovins, ovins et caprins. Besoins des animaux – Valeurs des aliments. Tables INRA 2010 (édition remaniée), J Agabriel (coord), pp.185-279.

Beaudoin, N., Launay, M., Sauboua, E., Ponsardin, G., Mary, B., 2008. Evaluation of the soil crop model STICS over 8 years against the "on farm" database of Bruyères catchment. Eur. J. Agron. 29, 46–57. https://doi.org/10.1016/j.eja.2008.03.001.

Bennett, E.M., Peterson, G.D., Gordon, L.J., 2009. Understanding relationships among multiple ecosystem services: relationships among multiple ecosystem services. Ecol. Lett. 12, 1394–1404. https://doi.org/10.1111/j.1461-0248.2009.01387.x.

Bennett, D., Harms, T.E., 2013. Crop Yield and Water Requirement Relationships for Major Irrigated Crops in Southern Alberta. Can. Water Resour. J./Revue canadienne des ressources hydriques 36, 159–170. https://doi.org/10.4296/cwrj3602853.

Bouma, J., 2010. Implications of the knowledge paradox for soil science. Adv. Agron. 106, 143–171.

Bouma, J., 2014. Soil science contributions towards Sustainable Development Goals and their implementation: linking soil functions with ecosystem services. Z. Pflanzenernähr. Bodenk. 177, 111–120. https://doi.org/10.1002/jpln.201300646.

Brisson, N., Gary, C., Justes, E., Roche, R., Mary, B., Ripoche, D., Zimmer, D., Sierra, J., Bertuzzi, P., Burger, P., Bussière, F., Cabidoche, Y.M., Cellier, P., Debaeke, P., Gaudillère, J.P., Hénault, C., Maraux, F., Seguin, B., Sinoquet, H., 2003. An overview of the crop model stics. Eur. J. Agron. 18, 309–332. https://doi.org/10.1016/S1161-0301(02)00110-7.

Calzolari, C., Ungaro, F., Filippi, N., Guermandi, M., Malucelli, F., Marchi, N., Staffilani, F., Tarocco, P., 2016. A methodological framework to assess the multiple contributions of soils to ecosystem services delivery at regional scale. Geoderma 261, 190–203. https://doi.org/10.1016/j.geoderma.2015.07.013.

Cardona, A., 2012. L'introduction de la notion de services écosystémiques pour un nouveau regard sur le sol. In: 6 éme Journées de Recherches En Sciences Sociales, p. 14.

Chen, S., Martin, M.P., Saby, N.P.A., Walter, C., Angers, D., Arrouays, D., 2018. Fine resolution map of top- and subsoil carbon sequestration potential in France. Sci. Total Environ. 630, 389–400. https://doi.org/10.1016/j.scitotenv.2018.02.209.

CICES, 2013. CICES V4.3 (January 2013). <http://www.cices.eu/>.

Clec'h, S.L., Oszwald, J., Decaens, T., Desjardins, T., Dufour, S., Grimaldi, M., Jegou, N., Lavelle, P., 2016. Mapping multiple ecosystem services indicators: toward an objective-oriented approach. Ecol. Ind. 69, 508–521. https://doi.org/10.1016/j.ecolind.2016.05.021.

Climatik., 2019. Climatik databases, INRA.

Costanza, R., d'Arge, R., de Groot, R., Farber, S., Grasso, M., Hannon, B., Limburg, K., Naeem, S., O'Neill, V.R., Paruelo, J., Raskin, R.G., Sutton, P., van den Belt, M., 1997. The value of the world's ecosystem services and natural capital. Nature 387, 253–260. https://doi.org/10.1038/387253a0.

Curtin, F., Schulz, P., 1998. Multiple correlations and bonferroni's correction. Biol. Psychiatry 44, 775–777. https://doi.org/10.1016/S0006-3223(98)00043-2.

de Groot, R.S., Alkemade, R., Braat, L., Hein, L., Willemen, L., 2010. Challenges in integrating the concept of ecosystem services and values in landscape planning, management and decision making. Ecol. Complexity 7, 260–272. https://doi.org/10.1016/j.ecocom.2009.10.006.

Deng, X., Li, Z., Gibson, J., 2016. A review on trade-off analysis of ecosystem services for sustainable land-use management. J. Geogr. Sci. 26, 953–968. https://doi.org/10.1007/s11442-016-1309-9.

Díaz, S., Pascual, U., Stenseke, M., Martín-López, B., Watson, R.T., Molnár, Z., Hill, R., Chan, K.M.A., Baste, I.A., Brauman, K.A., Polasky, S., Church, A., Lonsdale, M., Larigauderie, A., Leadley, P.W., van Oudenhoven, A.P.E., van der Plaat, F., Schröter, M., Lavorel, S., Aumeeruddy-Thomas, Y., Bukvareva, E., Davies, K., Demissew, S., Erpul, G., Failler, P., Guerra, C.A., Hewitt, C.L., Keune, H., Lindley, S., Shirayama, Y., 2018. Assessing nature's contributions to people. Science 359, 270–272. https://doi.org/10.1126/science.aap8826.

Dominati, E., Patterson, M., Mackay, A., 2010. A framework for classifying and quantifying the natural capital and ecosystem services of soils. Ecol. Econ. 69, 1858–1868. https://doi.org/10.1016/j.ecolecon.2010.05.002.

Dominati, E.J., Mackay, A., Lynch, B., Heath, N., Millner, I., 2014. An ecosystem services approach to the quantification of shallow mass movement erosion and the value of soil conservation practices. Ecosyst. Serv. 9, 204–215. https://doi.org/10.1016/j.ecoser.2014.06.006.

Drobnik, T., Greiner, L., Keller, A., Grêt-Regamey, A., 2018. Soil quality indicators – from soil functions to ecosystem services. Ecol. Ind. 94, 151–169. https://doi.org/10.1016/j.ecolind.2018.06.052.

Dray, S., Dufour, A.B., 2007. The ade4 package: implementing the duality diagram for ecologists. J. Stat. Softw. 22 (4), 1–20.

EFESE-EA, 2017. Rapport scientifique de l'etude réalisé par l'INRA-volet « écosystémes agricoles » de l'Evaluation Française des Ecosytémes et des Services Ecosystémiques,970 p.

Egoh, B., Reyers, B., Rouget, M., Richardson, D.M., Le Maitre, D.C., van Jaarsveld, A.S., 2008. Mapping ecosystem services for planning and management. Agric. Ecosyst. Environ. 127, 135–140. https://doi.org/10.1016/j.agee.2008.03.013.

Ellili-Bargaoui, Y., Malone, B.P., Michot, D., Minasny, B., Vincent, S., Walter, C., Lemercier, B., 2020. Comparing three approaches of spatial disaggregation of legacy soil maps based on the Disaggregation and Harmonisation of Soil Map Units Through Resampled Classification Trees (DSMART) algorithm. SOIL 6, 371–388. https://doi.org/10.5194/soil-6-371-2020.

Ellili Bargaoui, Y., Walter, C., Michot, D., Saby, N.P.A., Vincent, S., Lemercier, B., 2019. Validation of digital maps derived from spatial disaggregation of legacy soil maps. Geoderma 356, 113907. https://doi.org/10.1016/j.geoderma.2019.113907.

Ellili, Y., Walter, C., Michot, D., Pichelin, P., Lemercier, B., 2019. Mapping soil organic carbon stock change by soil monitoring and digital soil mapping at the landscape scale. Geoderma 351, 1–8. https://doi.org/10.1016/j.geoderma.2019.03.005.

European Commission, 2013. Available at <https://ec.europa.eu/regional_policy/sources/how/policy/doc/strategic_report/2013/strat_report_2013_en.pdf> .

FAO, 2003. Evaluation du bilan en éléments nutritifs du sol. Approches et méthodologies. FAO Fertilizer and Plant Nutrition Bulletin 14, Rome.

Fossey, M., Bustany, C., Angers, D., Cudennec, C., Durand, P., Gascuel, C., Jaffrezic, A., Pérès, G., Bois, S., Warot, G., Walter, C., 2020. A framework to consider soil ecosystem services in territorial planning. Front. Environ. Sci. 8, 28. https://doi.org/10.3389/fenvs.2020.00028.

Francesconi, W., Srinivasan, R., Pérez-Miñana, E., Willcock, S.P., Quintero, M., 2016. Using the Soil and Water Assessment Tool (SWAT) to model ecosystem services: a systematic review. J. Hydrol. 535, 625–636. https://doi.org/10.1016/j.jhydrol.2016.01.034.

Fu, Q., Li, B., Yang, L., Wu, Z., Zhang, X., 2015. Ecosystem services evaluation and its spatial characteristics in Central Asia's Arid Regions: a case study in Altay Prefecture, China. Sustainability 7, 8335–8353. https://doi.org/10.3390/su7078335.

Fraga, H., García de Cortázar Atauri, I., Santos, J.A., 2018. Viticultural irrigation demands under climate change scenarios in Portugal. Agric. Water Manag. 196, 66–74. https://doi.org/10.1016/j.agwat.2017.10.023.

Grace, J.B., 2006. Structural Equation Modeling and Natural Systems. Cambridge University Press, Cambridge, UK.

Greiner, L., Keller, A., Grêt-Regamey, A., Papritz, A., 2017. Soil function assessment: review of methods for quantifying the contributions of soils to ecosystem services. Land Use Policy 69, 224–237. https://doi.org/10.1016/j.landusepol.2017.06.025.

Grimaldi, M., Oszwald, J., Dolédec, S., Hurtado, M. del P., de Souza Miranda, I., Arnauld de Sartre, X., Assis, W.S. de, Castañeda, E., Desjardins, T., Dubs, F., Guevara, E., Gond, V., Lima, T.T.S., Marichal, R., Michelotti, F., Mitja, D., Noronha, N.C., Delgado Oliveira, M.N., Ramirez, B., Rodriguez, G., Sarrazin, M., da Silva, M.L. da, Costa, L.G. S., Souza, S.L., de Veiga, I., Velasquez, E., Lavelle, P., 2014. Ecosystem services of regulation and support in Amazonian pioneer fronts: searching for landscape drivers. Landscape Ecol. 29, 311–328. https://doi.org/10.1007/s10980-013-9981-y.

Hassink, J., 1992. Effects of soil texture and structure on carbon and nitrogen mineralization in grassland soils. Biol. Fertil. Soils 14, 126–134. https://doi.org/10.1007/BF00336262.

Hassink, J., 1997. The capacity of soils to preserve organic C and N by their association with clay and silt particles 2.

Hauck, J., Albert, C., Fürst, C., Geneletti, D., La Rosa, D., Lorz, C., Spyra, M., 2016. Developing and applying ecosystem service indicators in decision-support at various scales. Ecol. Ind. 61, 1–5. https://doi.org/10.1016/j.ecolind.2015.09.037.

INRA Infosol, 2014. Donesol Version 3.4.3. Dictionnaire de données.

IUSS Working Group WRB: World reference base for soil resources 2014. World Soil Resources Reports No. 103. FAO, Rome,116 pp.

Jopke, C., Kreyling, J., Maes, J., Koellner, T., 2015. Interactions among ecosystem services across Europe: bagplots and cumulative correlation coefficients reveal synergies, trade-offs, and regional patterns. Ecol. Ind. 53, 295–296. https://doi.org/10.1016/j.ecolind.2014.09.037.

Lee, H., Lautenbach, S., 2016. A quantitative review of relationships between ecosystem services. Ecol. Ind. 66, 340–351. https://doi.org/10.1016/j.ecolind.2016.02.004.

Maes, J., Paracchini, M.L., Zulian, G., Dunbar, M.B., Alkemade, R., 2012. Synergies and trade-offs between ecosystem service supply, biodiversity, and habitat conservation status in Europe. Biol. Conserv. 155, 1–12. https://doi.org/10.1016/j.biocon.2012.06.016.

Malik, A.A., Puissant, J., Buckeridge, K.M., Goodall, T., Jehmlich, N., Chowdhury, S., Gweon, H.S., Peyton, J.M., Mason, K.E., van Agtmaal, M., Blaud, A., Clark, I.M., Whitaker, J., Pywell, R.F., Ostle, N., Gleixner, G., Griffiths, R.I., 2018. Land use driven change in soil pH affects microbial carbon cycling processes. Nat. Commun. 9, 3591. https://doi.org/10.1038/s41467-018-05980-1.

Marraccini, E., Gotor, A.A., Scheurer, O., Leclercq, C., 2020. An innovative land suitability method to assess the potential for the introduction of a new crop at a regional level. Agronomy 10, 330.

MEA, 2005. Millenium ecosystem assessment. Ecosystems and human well-being: biodiversity synthesis. World Resources Institute, Washington, DC.

McBratney, A., Field, D.J., Koch, A., 2014. The dimensions of soil security. Geoderma 213, 203–213. https://doi.org/10.1016/j.geoderma.2013.08.013.

Meynard, J.-M., Cerf, M., Guichard, L., Jeuffroy, M.-H., Makowski, D., 2002. Which decision support tools for the environmental management of nitrogen? Agronomie 22, 817–829. https://doi.org/10.1051/agro:2002064.

Millennium Ecosystem Assessment, 2005. In: Ecosystems and Human Well-being: Biodiversity Synthesis. World Resources Institute, Washington, DC, p. 86.

Mouchet, M.A., Lamarque, P., Martín-López, B., Crouzat, E., Gos, P., Byczek, C., Lavorel, S., 2014. An interdisciplinary methodological guide for quantifying associations between ecosystem services. Global Environ. Change 28, 298–308. https://doi.org/10.1016/j.gloenvcha.2014.07.012.

Nelson, E., Mendoza, G., Regetz, J., Polasky, S., Tallis, H., Cameron, Dr, Chan, K.M., Daily, G.C., Goldstein, J., Kareiva, P.M., Lonsdorf, E., Naidoo, R., Ricketts, T.H., Shaw, Mr, 2009. Modeling multiple ecosystem services, biodiversity conservation, commodity production, and tradeoffs at landscape scales. Front. Ecol. Environ. 7, 4–11. https://doi.org/10.1890/080023.

Nemec, K.T., Raudsepp-Hearne, C., 2013. The use of geographic information systems to map and assess ecosystem services. Biodivers. Conserv. 22, 1–15. https://doi.org/10.1007/s10531-012-0406-z.

O'Geen, A.T., 2012. Soil Water Dynamics. Nat. Educ. Knowl. 3 (6), 12.

Qin, K., Li, J., Yang, X., 2015. Trade-Off and Synergy among Ecosystem Services in the Guanzhong-Tianshui Economic Region of China. Int. J. Environ. Res. Public Health 12, 14094–14113. https://doi.org/10.3390/ijerph121114094.

R Core Team, 2019. R: A Language and Environment for Stati stical Computing. R. Foundation for Statistical Computing, Vienna, Austria 3-900051-07-0. <http://www.R-project.org>.

Raudsepp-Hearne, C., Peterson, G.D., Bennett, E.M., 2010. Ecosystem service bundles for analyzing tradeoffs in diverse landscapes. Proc. Natl. Acad. Sci. 107, 5242–5247. https://doi.org/10.1073/pnas.0907284107.

Remy, A., Walter, C., Lemercier, B., 2015. Développement des fonctions de Pedotransfert pour prédire les états d'humidité des sols en Bretagne. In Sols de Bretagne rapport, Agrocampus-ouest-INRA.

Robinson, D.A., Emmett, B.A., Reynolds, B., Rowe, E.C., Spurgeon, D., Keith, A.M., Lebron, I., Hockley, N., 2012. Chapter 3. soil natural capital and ecosystem service delivery in a world of global soil change. In: Hester, R.E., Harrison, R.M. (Eds.), Issues in Environmental Science and Technology. Royal Society of Chemistry, Cambridge, pp. 41–68. https://doi.org/10.1039/9781849735438-00041.

Rousseeuw, P.J., Ruts, I., Tukey, J.W., 1999. Statistical computing and graphics: the bagplot: a bivariate boxplot. Am. Stat. 382–387.

Silva, F.A.M., Naudin, K., Corbeels, M., Scopel, E., Affholder, F., 2019. Impact of conservation agriculture on the agronomic and environmental performances of maize cropping under contrasting climatic conditions of the Brazilian Cerrado. Field Crops Res. 230, 72–83. https://doi.org/10.1016/j.fcr.2018.10.009.

Singh, M., Sarkar, B., Sarkar, S., Churchman, J., Bolan, N., Mandal, S., Menon, M., Purakayastha, T.J., Beerling, David.J, 2017. Stabilization of soil organic carbon as influenced by clay mineralogy. Adv. Agron. 53.

Szabolcs, I, 1994.The concept of soil resilience. Soil resilience and sustainable land use. In: Greenland, D.J. and Szabolcs, I., Eds., CAB International and Willingford, 33-39.

TEEB, 2010. Mainstreaming the economics of nature: a synthesis of the approach, conclusions and recommendations of teeb, The economics of ecosystems & biodiversity. UNEP, Geneva.

Tomscha, S.A., Gergel, S.E., 2016. Ecosystem service trade-offs and synergies misunderstood without landscape history. Ecol. Soc. 21 https://doi.org/10.5751/ES-08345-210143.

Tukey, J.W., 1975. Mathematics and the picturing of data. Proc.In. Congress Math., Vancouver 2, 523-531.

United Nations Sustainable Development Goals 2015 <https://www.sustainabledevelopment.un.org>.

Vallet, A., Locatelli, B., Levrel, H., Wunder, S., Seppelt, R., Scholes, R.J., Oszwald, J., 2018. Relationships between ecosystem services: comparing methods for assessing tradeoffs and synergies. Ecol. Econ. 150, 96–106. https://doi.org/10.1016/j.ecolecon.2018.04.002.

Van Wijnen, H.J., Rutgers, M., Schouten, A.J., Mulder, C., de Zwart, D., Breure, A.M., 2012. How to calculate the spatial distribution of ecosystem services — natural attenuation as example from The Netherlands. Sci. Total Environ. 415, 49–55. https://doi.org/10.1016/j.scitotenv.2011.05.058.

Vincent, S., Lemercier, B., Berthier, L., Walter, C., 2018. Spatial disaggregation of complex Soil Map Units at the regional scale based on soil-landscape relationships. Geoderma 311, 130–142. https://doi.org/10.1016/j.geoderma.2016.06.006.

Vrebos, D., Staes, J., Vandenbroucke, T., D'Haeyer, R., Johnston, R., Muhumuza, M., Kasabeke, C., Meire, P., 2015. Mapping ecosystem service flows with land cover scoring maps for data-scarce regions. Ecosyst. Serv. 13, 28–40. https://doi.org/10.1016/j.ecoser.2014.11.005.

Wu, J., Feng, Z., Gao, Y., Peng, J., 2013. Hotspot and relationship identification in multiple landscape services: a case study on an area with intensive human activities. Ecol. Ind. 29, 529–537. https://doi.org/10.1016/j.ecolind.2013.01.037.

Zheng, Z., Fu, B., Hu, H., Sun, G., 2014. A method to identify the variable ecosystem services relationship across time: a case study on Yanhe Basin, China. Landsc. Ecol. 29, 1689–1696. https://doi.org/10.1007/s10980-014-0088-x.